

PEOPLE'S DEMOCRATIC REPUBLIC OF ALGERIA  
MINISTRY OF HIGHER EDUCATION AND SCIENTIFIC RESEARCH  
ECHAHID CHEIKH LARBI TEBESSI UNIVERSITY-TEBESSA  
FACULTY OF EXACT SCIENCES AND THE SCIENCES OF NATURE  
AND LIFE  
DEPARTMENT OF MATTER SCIENCES



Memory of MASTER  
Specialty: Physics of materials

Effect of Cu doping on optical and electrical properties of  
ZnO thin films deposited by spray pyrolysis technique

Presented by:

**Wafa LEMOUCHI**

Members of jury:

Souheila ZOUAI	MCA	President	Echahid Cheikh Larbi Tebessi
Labidi HERISSI	MCA	Supervisor	Echahid Cheikh Larbi Tebessi
Abdelkader HAFDALLAH	MCA	Examiner	Echahid Cheikh Larbi Tebessi

University season: 2022/2023

PEOPLE'S DEMOCRATIC REPUBLIC OF ALGERIA

MINISTRY OF HIGHER EDUCATION AND SCIENTIFIC RESEARCH

ECHAHID CHEIKH LARBI TEBESSI UNIVERSITY-TEBESSA

FACULTY OF EXACT SCIENCES AND THE SCIENCES OF NATURE  
AND LIFE

DEPARTMENT OF MATTER SCIENCES



**Memory of MASTER**

Specialty: **Physics of materials**

**Effect of Cu doping on optical and electrical properties of  
ZnO thin films deposited by spray pyrolysis technique**

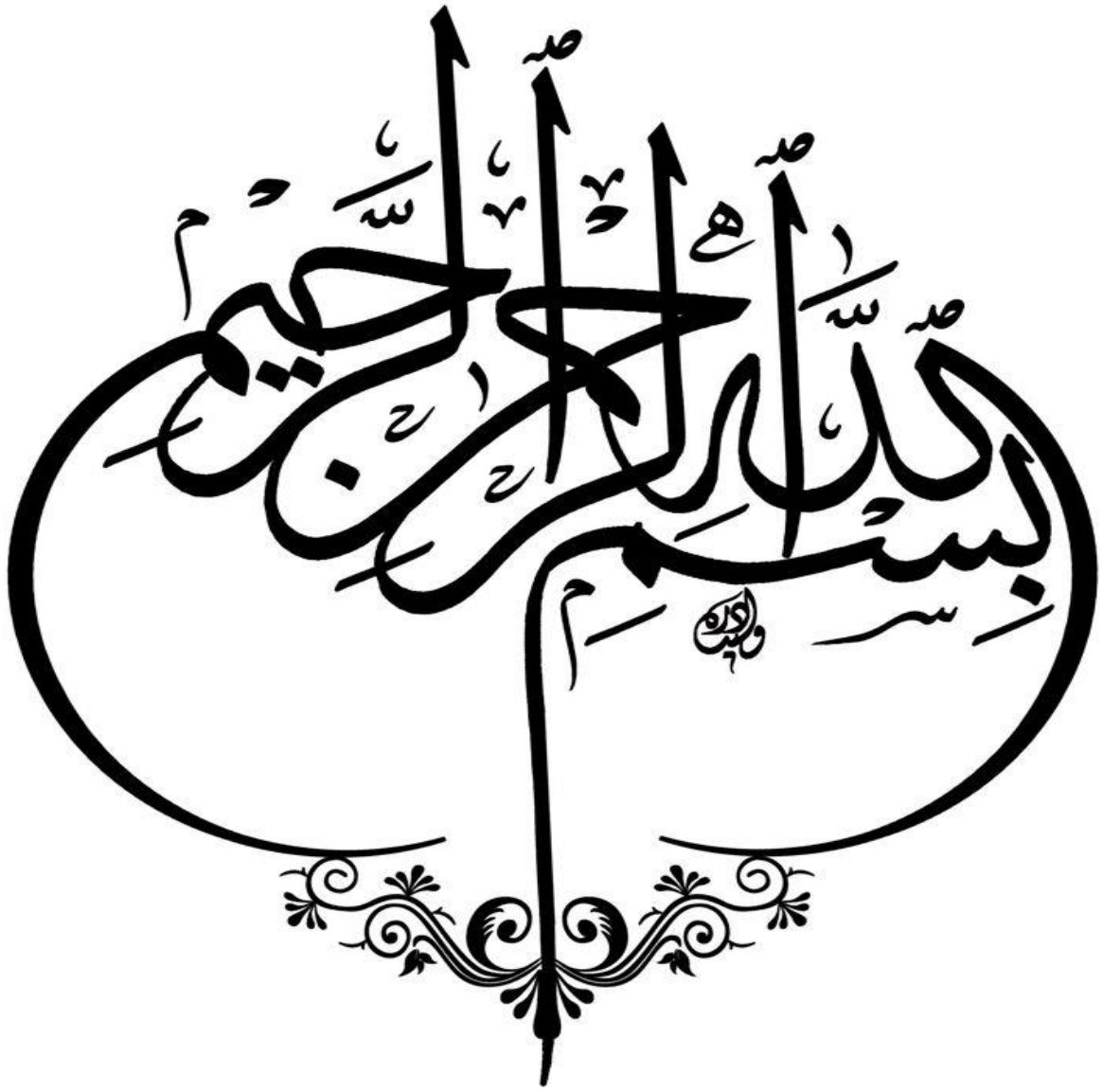
Presented by:

**Wafa LEMOUCHI**

Members of jury:

Souheila ZOUAI	MCA	President	Echahid Cheikh Larbi Tebessi
Labidi HERISSI	MCA	Supervisor	Echahid Cheikh Larbi Tebessi
Abdelkader HAFDALLAH	MCA	Examiner	Echahid Cheikh Larbi Tebessi

University season: 2022/2023



« يَرْفَعِ اللَّهُ الَّذِينَ آمَنُوا مِنْكُمْ وَالَّذِينَ أُوتُوا الْعِلْمَ دَرَجَاتٍ »

المجادلة - الآية 11

## ACKNOWLEDGEMENTS

Firstly, I thank **GOD** the whole powerful for having agreed his infinite kindness, courage, the force and patience to complete this modest work. After that, I make a point of profoundly thanking to my supervisor Dr. **Labidi HERISSI**, for his help, support, guidance and encouragement. He has been a great support on all fronts and made my memory journey a memorable experience.


We would like to thank Ms. **Souheila ZOUAI** and Mr. **Abdelkader HAFDALLAH** for having participated in the evaluation of this work.

We warmly thank Pr. **Lazhar HADJERIS**, Director of the Laboratory of Materials and Structure of Electromechanical Systems and their Reliability (LMSSEF) at Larbi Ben M'hidi University of Oum El Bouaghi for his welcome and his help which contributed to carrying out this term work. Finally, we appreciate anybody who helps directly or indirectly to my final year project. I want to express my appreciation of the comments and recommendations that have been vital to the accomplishment of this study.



# Dedication

Firstly, I thank those who favored them. My beloved parents do not cease to me for all their efforts from the moment of my birth to these blessed moments. I thank my sisters because they were the source of support, advice, guidance and contributed. To my companion the best friend Dr. Bahia Ghenaiet and my colleagues Aya, Lynda.



**TABLE OF CONTENTS**

List of figures ..... I  
List of tables..... III  
List of symbols..... IV  
List of abbreviations..... V  
General introduction..... 1

**Chapter I: Generalities about zinc oxide and copper oxide thin films**

I.1. Transparent conductive oxides ..... 3  
    I.1.1. Definition ..... 3  
    I.1.2. The necessary properties of TCO ..... 3  
        I.1.2.1. Structural properties of TCO ..... 3  
        I.1.2.2. Electrical properties of TCO..... 4  
        I.1.2.3. Optical properties of TCO..... 5  
    I.1.3. TCO doping ..... 6  
I.2. Zinc oxide ..... 7  
    I.2.1. Properties of zinc oxide ..... 7  
        I.2.1.1. Crystallographic properties of ZnO..... 7  
        I.2.1.2. Piezoelectricity properties of ZnO..... 9  
        I.2.1.3. Optical properties of ZnO..... 10  
        I.2.1.4. Electrical properties of ZnO ..... 10  
        I.2.1.5. Catalytic and chemical properties of ZnO..... 10  
    I.2.2. ZnO applications..... 11  
    I.2.3. Choice of dopants ..... 11  
I.3. Copper oxides ..... 11  
    I.3.1. Cuprous oxide..... 11  
    I.3.2. Cupric oxide ..... 13  
I.4. What are thin films?..... 13  
I.5. Classification of growth patterns..... 14

# Table of contents

I.5.1. Island growth.....	14
I.5.2. Layered growth.....	14
I.5.3. Mixed growth.....	14
I.6. Thin films preparation Techniques.....	15
I.6.1. Physical process.....	15
I.6.1.1. In the vacuum middle .....	15
a. Laser ablation method.....	16
b. Joule effect method.....	16
I.6.1.2. In the plasma middle .....	17
I.6.2. Chemical process.....	17
I.6.2.1. Chemical vapor deposition.....	17
I.6.2.2. Chemical solution deposition.....	18
a. Sol–Gel Method.....	18
b. Chemical bath deposition method.....	19
c. Spray pyrolysis method.....	20

## **Chapter II: Preparation of copper-doped zinc oxide thin films and analysis techniques**

<b>Part one:</b> Elaboration copper-doped zinc oxide thin films.....	22
II.1. Ultrasonic spray pyrolysis technique .....	22
II.1.1. Stages of forming thin films by spray pyrolysis technique.....	22
II.1.2. What are the advantages of spray pyrolysis?.....	23
II.1.3. Factors affecting thin film preparation by ultrasonic spray pyrolysis technique.....	23
II.1.3.1. Atomization rate and droplet size.....	23
II.1.3.2. Effect of Substrate temperature.....	23
II.1.3.3. Effect of deposit time.....	24
II.1.3.4. Effect of the nozzle-substrate distance.....	24
II.2. Experimental procedure.....	25
II.3. Followed equipment.....	25
II.4. Stages of preparation thin films.....	26
II.4.1. Choice the substrate.....	27
II.4.2. Preparation the substrate.....	27

# Table of contents

II.4.3. Preparation of deposition solution.....	28
II.4.3.1. Preparation the solution of zinc acetate dihydrate.....	28
II.4.3.2. Preparation the solution of copper chloride dihydrate.....	28
II.4.3.3. Preparation the solution of precursor.....	29
II.4.4. Thin films preparation.....	29
<b>Part two: Characterization techniques of thin films.....</b>	<b>30</b>
II.1. Optical characterization of thin films.....	30
II.1.1. Determination of film thickness and refractive index.....	31
II.1.2. Determination of absorption coefficient and optical band gap.....	31
II.1.3. Determination of Urbach Energy.....	32
II.2. Electrical characterization of thin films.....	33
 <b>Chapter III: Results and discussion</b>	
III.1. Photos of our samples.....	36
III.2. Effect the doping with Cu and the distance on the thickness of ZnO thin films.....	37
III.3. Effect the doping with Cu and the distance on the optical transmittance of ZnO thin films.....	38
III.4. Effect the doping with Cu and the distances on the optical band gap of ZnO thin films.....	42
III.5. Effect the doping with Cu and distance on the Urbach energy of ZnO thin films.....	43
III.6. Effect the doping with Cu and the distance on the refractive index of ZnO thin films.....	45
III.7. Effect the doping with Cu and the distance on the electrical conductivity of ZnO thin films.....	47
<b>General conclusion.....</b>	<b>49</b>
References.....	50



## List of figures

Figure No.	Title	Page
I.1	The three possible electrical states	4
I.2	Transmission, reflection and absorption spectra of a TCO sample	5
I.3	type-n Doping	6
I.4	type-p Doping	7
I.5	Crystal structure of ZnO rock-salt and zinc blende	8
I.6	Photo of a zincite crystal and crystal structure of hexagonal wurtzite ZnO	8
I.7	Illustration of the behavior of a piezoelectric pellet	9
I.8	Number of publications with the keyword of cuprous oxide in their title on the science direct website page from 2000 to 2022	12
I.9	The crystal structure of Cu <sub>2</sub> O	12
I.10	Schematic representation of the crystallographic structure of CuO	13
I.11	Basic Modes of thin film growth	14
I.12	Classification of thin film deposition techniques	15
I.13	The pulsed laser deposition (PLD) method	16
I.14	Schematic of Joule effect technique	17
I.15	Schematic model describing the film formation during the dip-coating process	19
I.16	Schematic model describing the film formation during the spin-coating process	19
I.17	Chemical bath deposition technique.	20
I.18	Spray pyrolysis method using, Pneumatic, and Ultrasonic	21
II.1	Effect of substrate temperature on the formation of thin films	24
II.2	Effect of Nozzle-Substrate distance on film elaboration	25
II.3	Equipment used in ultrasonic spray pyrolysis technique	26
II.4	Schematize Ultrasonic Spray Pyrolysis (USP)	26
II.5	Description of the cleaning process	27
II.6	Zinc acetate dihydrate as powder and as solution	28
II.7	Stage of preparation of copper chloride solution	29
II.8	Copper chloride dihydrate as powder and as solution	29
II.9	Preparation the precursor solution	29

## List of figures

<b>II.10</b>	Principle of measure the transmission UV-Vis and transmission spectrum example of copper and zinc oxide thin films	31
<b>II.11</b>	Explanation of band gape	32
<b>II.12</b>	Determination of Urbach energy	33
<b>II.13</b>	Diagram representing the principle of the four-point method	34
<b>II.14</b>	Four-point device	34
<b>III.1</b>	Photos of thin films deposited on glass substrates.	36
<b>III.2</b>	Variation the luminosity with different Cu concentration of the Samples	37
<b>III.3</b>	Variation of average film thickness of ZnO as a function Cu concentration at two different distances	38
<b>III.4</b>	Optical transmittance spectra of ZnO:Cu samples prepared at $d_{N-S} = 4$ cm and $d_{N-S} = 6$ cm	39
<b>III.5</b>	Optical transmittance spectra of ZnO:Cu thin films prepared at $d_{N-S} = 4$ cm and $d_{N-S} = 6$ cm	40
<b>III.6</b>	Schematic diagram shows the solution spray from the nozzle to substrate.	41
<b>III.7</b>	Variation of optical transmission of ZnO:Cu (8 at.%) thin films at two different Nozzle-Substrate distances	42
<b>III.8</b>	Variation the optical gap energy of ZnO thin films as a function of Cu concentration at two different distances	42
<b>III.9</b>	Variation the Urbach energy of ZnO thin films as a function of Cu concentration at two different distances	43
<b>III.10</b>	Variation of Urbach energy and gap energy of ZnO thin films as a function of Cu-doping percentage in 4cm and 6cm	45
<b>III.11</b>	Variation the refractive index of ZnO thin films as a function of Cu concentration at two different distances	46
<b>III.12</b>	Variation of thickness and refractive index of ZnO thin films versus Cu concentration prepared at 4cm and 6cm	46
<b>III.13</b>	Variation of electrical conductivity of ZnO:Cu thin films at two different distances	47

# List of tables

## List of tables

<b>Table No.</b>	<b>Title</b>	<b>Page</b>
<b>I.1</b>	Examples of doping some TCOs	7
<b>I.2</b>	Some characteristics and configuration of the mesh hexagonal ZnO	8
<b>I.3</b>	Some optical properties of ZnO	10
<b>III.1</b>	Optical transmittance ZnO:Cu at 600 nm	41

## List of symbols

### List of symbols

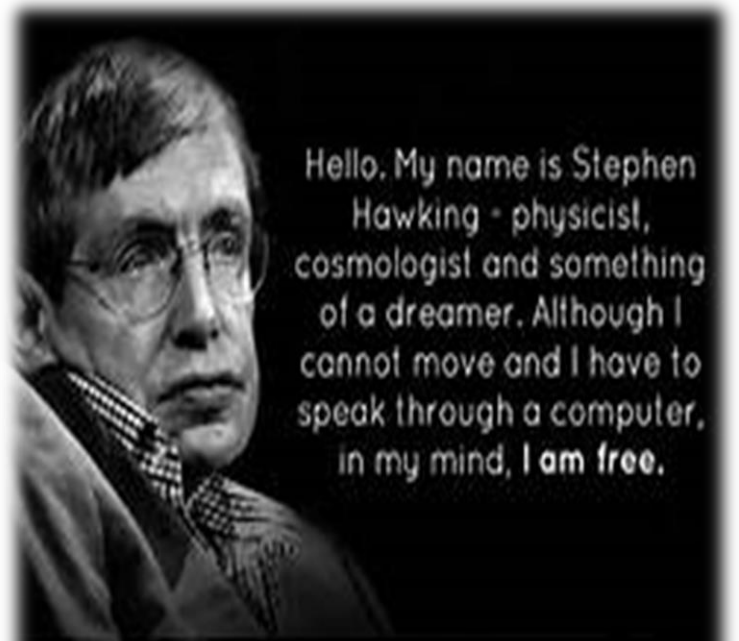
Symbol	Signification	Unit
$M$	Mass molar	$g / mol$
$C$	Solution concentration	$mol / l$
$m$	Mass	$g$
$V$	Volume	$l$
$d_{N-S}$	Distance between nozzle and substrate	$cm$
$T$	Temperature	$^{\circ}C$
$\alpha$	Absorption coefficient	$cm^{-1}$
$n$	Refractive index	
$E_g$	Energy of optical band gap	$eV$
$T$	Optical transmittance	%
$I$	Intensity of light	$W/m^2$
$d$	Film thickness	$nm$
$\lambda$	Wavelength of incident photon	$nm$
$\varphi_s$	Spray flow rate	$ml / h$
$h\nu$	Energy of incident photon	$eV$
$E_{Urb}$	Urbach energy	$eV$
$I$	Electrical current	$A$
$V$	Voltage	$V$
$\rho_s$	Surface resistivity	$\Omega / sqr$
$\sigma$	Electrical conductivity	$\Omega^{-1}.cm^{-1}$

## List of abbreviation

### List of abbreviation

ZnO	Zinc oxide
CuO	Cupric oxide
Cu <sub>2</sub> O	Cuprous oxide
ZnO:Cu	Copper-doped zinc oxide
<i>PLD</i>	Pulsed-laser deposition
<i>DC</i>	direct current
<i>RF</i>	radio frequency
<i>CVD</i>	Chemical vapor deposition
<i>PECVD</i>	Plasma Enhanced Chemical Vapor Deposition
<i>MOCVD</i>	Metal-Organic Chemical Vapor Deposition
<i>LPCVD</i>	Low Pressure Chemical Vapor Deposition
<i>Sol – Gel</i>	Solution-gelling
<i>TCOs</i>	transparent conducting oxides
Zn(CH <sub>3</sub> COO) <sub>2</sub> ·2H <sub>2</sub> O	zinc acetate dihydrate
(CuCl <sub>2</sub> · 2H <sub>2</sub> O)	copper chloride dihydrate
V <sub>ZAD</sub>	Volume of zinc acetate dihydrate
V <sub>CCD</sub>	Volume of copper chloride dihydrate
<i>UV – Vis – NIR</i>	Ultraviolet-visible-near infrared

# General introduction



## General introduction

The development of humanity has led to a sharp increase in energy consumption at the present time, which made some international organizations search (IOS) for a clean, easy and inexpensive source in the production of advanced energy like the solar cells means to meet this need [1], they found these advantages of transparent conductive oxides (TCO) in the form of thin films, and they were used in many applications from heat mirror window-coatings, which control the transmission of infrared energy into and out of buildings, to their use as the touch-screen technology, flat panel displays and gas sensors,...etc [2].

The interest in the form of thin films is related to its construction, which has over the past few years to improve their performance and expand their field of application, by making an advanced deposition machine to ensure obtaining materials with excellent electrical and optical properties [3]. These properties helped shed light on thin films and received many studies on them.

Zinc oxide (ZnO) is a transparent transition metal oxide in the visible whose refractive index in bulk form is equal to 2, n-type II-VI semiconductor, it has a wide gap direct (3.3 eV) and a large exciton binding energy (60 meV). The stable phase of ZnO is the hexagonal compact structure (hc) [4]. It has optical, electrical and electronic properties of interest for optoelectronic applications like to field UV photo-detectors [5].

Copper oxide is a semiconductor with two stable forms; cuprous oxide ( $\text{Cu}_2\text{O}$ ) and cupric oxide (CuO) has a cubic and monoclinic structure, respectively. These oxides have a large direct optical gap, of 1.2 eV for CuO and 2.1 eV for  $\text{Cu}_2\text{O}$  [6,7]. Allowing the absorption of visible light, can be used profitably in as many fields as ZnO without neglecting its non-toxic, it remains very versatile and efficient in the field of photo-catalysts and photo-degradation of organic dyes [8].

The properties of thin films of zinc oxide and copper oxide are highly dependent on the geometry and the specific growth technique and the elaboration conditions [8]. There are several ways to prepare it, physical pulsed-laser deposition [9] and chemical like to spray pyrolysis technique it is one of the most cost-effective methods for preparing thin films due to its ability to deposit a large uniform area, low manufacturing cost, simplicity, and low deposition temperature [10,11].

## General introduction

The purpose of this work is the elaboration of thin films onto glass substrates heated at 300°C, by ultrasonic spray pyrolysis technique, from precursor solution of zinc acetate dihydrate and copper chloride dihydrate at two different nozzle-substrate distances , and the study of the effect of the doping by Cu and nozzle-substrate distance on the properties of ZnO thin films, the deposit was made at the level of laboratory of material and structure of electromechanically systems and their reliability (LMSSEF: *Laboratoire des Matériaux et Structure des Systèmes électromécaniques et leur Fiabilité*) of Larbi Ben M'hidi University of Om El Bouaghi. These prepared slides were studied the optical properties using a UV-visible spectrophotometry and the electrical properties using four-point probe.

This memory organized in three chapters:

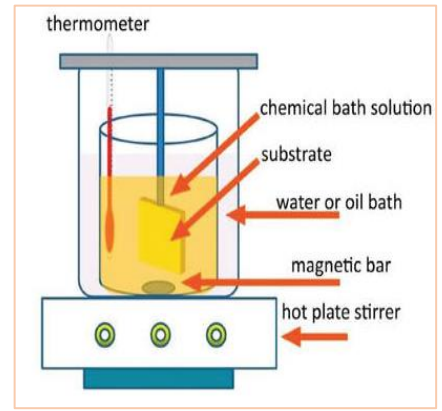
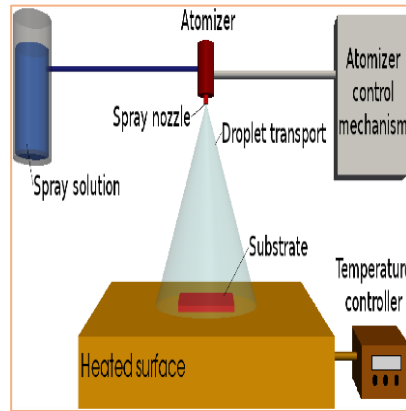
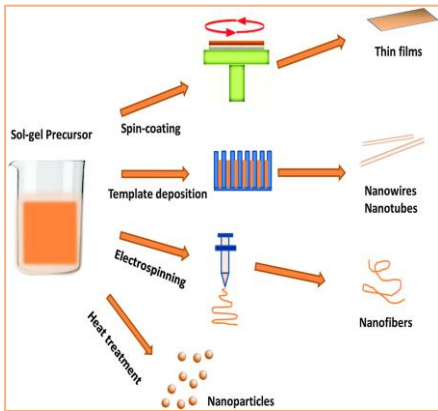
In the first chapter, we will look at a simplified explanation of the transparent conducting oxides because they are the most important elements for creating thin films. Then an overview of these films was presented, and the focus was on the basic properties of zinc oxide and copper oxide and its field of applications because it is the focus of the study. Next, the methods of preparing these films and focusing on spray pyrolysis technique.

The second chapter is devoted to the elaboration of zinc oxide thin films as well as the various experimental techniques to characterize our coatings.

In the third chapter, we present the discussions of the experimental results obtained of copper-doped zinc oxide thin films.

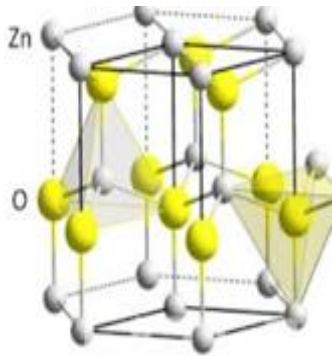
At the end, we conclude our work with general conclusion that summarizes the different steps and results achieved in this work.



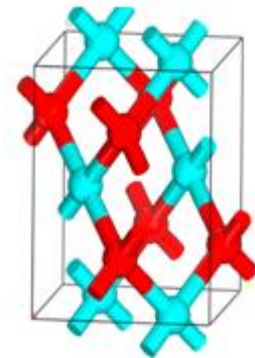


# Chapter I

Generalities about zinc oxide and copper oxide thin films



ZnO:Cu  
Thin films



## Chapter I: Generalities about zinc and copper oxide thin films

In this chapter, generally the focus was on the study of transparent conducting oxides, the most important element in this study was the optical and electrical properties, as well as the stacking the crystal structure and the electronic band structure of both zinc and copper oxides. Finally, been displayed a description the file different processes in producing the thin films.

### I.1. Transparent conductive oxides

#### I.1.1. Definition

Transparent conductive oxides (TCOs) are binary or triple compounds, which contain one or more of the metallic elements, consisting the metal atoms and atoms of oxygen ( $M_1xM_2yO_z$ ), where M is the chemical symbol of the Metal atom considered, O the symbol of the oxygen atom, “x “and “y “and “z “natural whole numbers [6]. for examples:

- Aluminum Oxide:  $Al_2O_3$ .
- Zinc Oxide: ZnO.
- Copper Oxides: CuO.
- Iron Oxides:  $Fe_2O_3$ .
- Tin oxide:  $SnO_2$ .

Conductive transparent oxides forma class of materials combining two properties: electrical conduction and transmittance in the visible range of light [12]. TCOs are used in several areas of application. So, Therefore, they are found in drones’ aircraft, satellite networks, flat screens, anti-freeze windows, heat-reflecting windows (Buildings, ovens, etc.), electromagnetic shields, electrostatic charge dissipators, photovoltaic cells and modules [12].

#### I.1.2. The necessary properties of TCO

##### I.1.2.1. Structural properties of TCO

Under the theory of energy bands, substances found in nature are classified into three main categories classes: conductors, insulators, and semiconductors (Figure I.1). In the case of metals, the conduction band (CB) and the valence band (VB) are overlapped, and this allows free movement of electrons, while in Semiconductors There is a forbidden band on the electrons that separates the conduction band on the valence band, called the energy gap and symbolized by  $E_g$ . In the event that the energy gap exceeds 5 eV, then was talking about insulators [9].

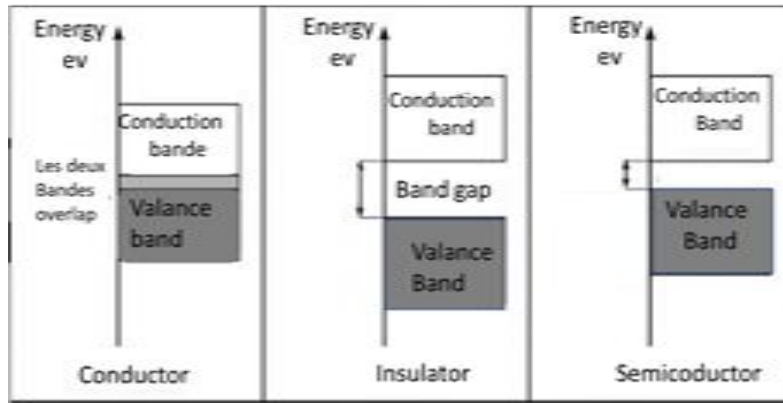


Figure I.1. The three possible electrical states [13].

### I.1.2.2. Electrical properties of TCO

The electrical properties of TCOs have been studied since 1970. If we say an electrical property, the first thing that comes to our mind is electrical conductivity, and it is also described through kinetics [14].

#### a. Conductivity

The transparent conducting oxides are characterized by a wide energy gap, in addition to the electrical conductivity within the limits  $10^{-3} - 10^{-4} (\Omega^{-1} \cdot \text{cm}^{-1})$  [15]. The latter depends on the concentration and density of electrons in the thin film, as well as on the mobility of these electrons, and it is given by the formula:

$$\sigma = \frac{1}{\rho} = e \cdot \mu \cdot n \quad (\text{I.1})$$

Where:

$\sigma$  : is the electrical conductivity  $\Omega^{-1} \cdot \text{cm}^{-1}$ ,

$\rho$  : is the electrical resistivity in  $\Omega \cdot \text{cm}$ ,

$n$ : is the electron density in the conduction band at  $\text{cm}^{-3}$ ,

$\mu$  :is their mobility in  $\text{cm}^2 \cdot \text{V}^{-1} \cdot \text{s}^{-1}$ ,

$e$ : is the load of electron,

#### b. Mobility

Another possibility to increase the electrical conductivity is to increase the mobility. However, mobility is intrinsically dependent on diffusion mechanisms and therefore cannot be controlled directly. In general, these mechanisms limit the mobility when the concentration of

carriers increases. As mentioned earlier, the mobility is essential for a good conductivity of the TCOs, the mobility is given by the formula [1,14]:

$$\mu = \frac{e \cdot \tau}{m^*} \tag{I.2}$$

Where:

$m^*$  :is the effective mass of the electron,

$\tau$  : is the average time between two collisions.

**I.1.2.3. Optical properties of TCO**

The optical properties of materials are governed by three essential phenomena (Figure I.2) that are the transmission T (Transmittance), the reflection R (Reflectance) and absorption A (absorbance) [16].

- The transmission factor is defined as being the ratio between the intensity of the transmitted light ( $\phi_T$ ) through a material with respect to the intensity of light incident on its surface ( $\phi_0$ ). ( $T = \frac{\phi_T}{\phi_0}$ ).
- The reflection factor is the intensity of the light which is reflected at the level of its surface ( $\phi_R$ ) by relative to the incident light intensity ( $\phi_0$ ) ( $R = \frac{\phi_R}{\phi_0}$ ).
- The absorption factor is the ratio between the intensity of the absorbed light ( $\phi_A$ ) and the intensity incident light ( $\phi_0$ ) ( $A = \frac{\phi_A}{\phi_0}$ ).

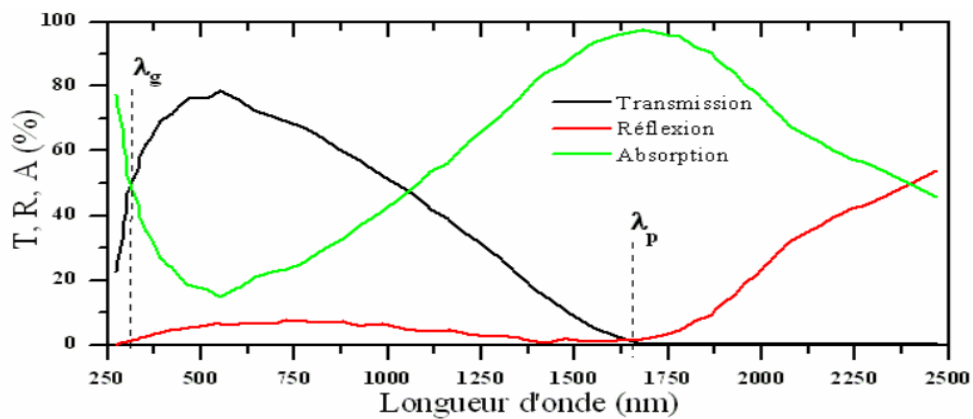


**Figure I.2.** Transmission, reflection and absorption spectra of a TCO sample [17].

**I.1.3. TCO Doping**

The charge carriers are usually generated by doping the insulator with suitable dopants and by defects. It is no wonder that this unique material property makes TCOs an important materia

property makes TCOs an important material in technology and useful in commercial applications [2].

In order to improve the electrical properties such as the number of charge carriers and the electrical conductivity which are modified by doping. Depending on the material or type of dopant (Table I.1), the doping can be substitution, vacation or interstitial implantations. Doping will induce the type of conduction (n or p) which depends on the valence of the dopants or the sites of implantations, acceptors or donors [18]. There are two types of doping:

### I.1.3.1. n-type doping

n-type semiconductor is an intrinsic semiconductor in which we have introduced donor-type impurities. The semiconductor is said to be doped. The materials thus formed are called n-type semiconductors because they contain an excess of electrons [17,19]. The introduction of electron donor atoms results in the appearance of a pseudo energy level located just below the conduction band (Figure I.3). Thereby, the energy required for electrons to pass into the conduction band is much greater easily achieved than in an intrinsic semiconductor [17].

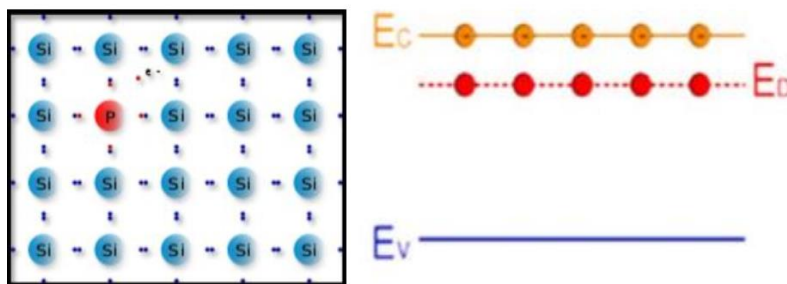


Figure I.3. n-type Doping.

### I.1.3.2. p-type doping

p-type doping consists of increasing the density of holes in the semiconductor (extrinsic semiconductor). To do this, we include a certain number of atoms poor in electrons in the semiconductor to create an excess of holes. In the example of silicon (Figure I.4), a trivalent atom is added (column III of the periodic table) [14,20].

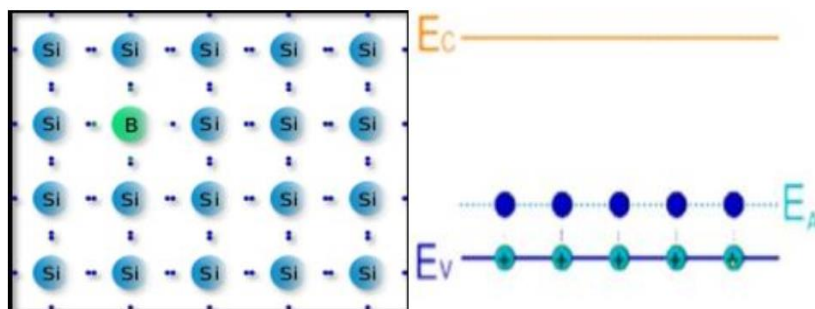


Figure I.4. p-type doping.

Table I.1. Examples of doping some TCOs.

Doping TCO	
n-type	p-type
ZnO: Cu, Cr, B, Al, Ga, Si	In <sub>2</sub> O <sub>3</sub> : Ag
In <sub>2</sub> O <sub>3</sub> : Sn, Ti, Zr, F	CuO: Ni
SnO <sub>2</sub> : Sb, As, P	CuO: Zn

## I.2. Zinc oxide (ZnO)

Zinc oxide (ZnO), is an II–VI semiconductor and an inorganic compound also known as calamine or white zinc, and it is a good semiconductor material [16]. It has been studied extensively since beginning in the 1950s before being relatively neglected in the 1970s, to find out then a huge revival of interest from the 90's due to its characteristics very attractive basics [21].

### I.2.1. Properties of zinc oxide

#### I.2.1.1. Crystallographic properties of ZnO

Zinc oxide, known in its natural state, exists in three crystallographic forms: the zinc blend form (Figure I.5.a), the cubic form (Rock-salt) (Figure I.5.b), and the hexagonal (Wurtzite) (Figure I.6.b). Blende form obtained only in the case of growth on cubic substrates. The structure of rock-salt, it is obtained only under high pressures under standard deconditions [12,22].

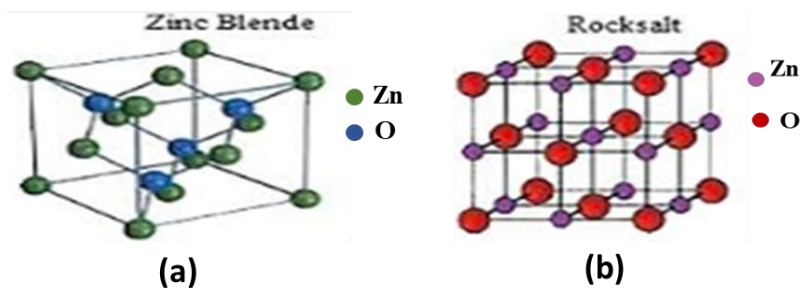


**Figure I.5.** Crystal structure of (a) zinc blende (b) ZnO rock-salt and.

The stable phase of ZnO (Zincite) is the hexagonal wurtzite structure (Figure I.6.a). It is made up layers of zinc atoms alternating with layers of oxygen atoms along the  $c$  axis compounds of  $\text{O}^{-2}$  and  $\text{Zn}^{+2}$  ions coordinated in tetrahedral form (Figure I.6.b). All atoms have the tetrahedral coordination with four nearest neighbors of the typical opposite. He is an isotropic whose preferred axis of crystal growth is the  $c$  axis. Its structure can be described as two hc networks that are inserted into each other [18,23].

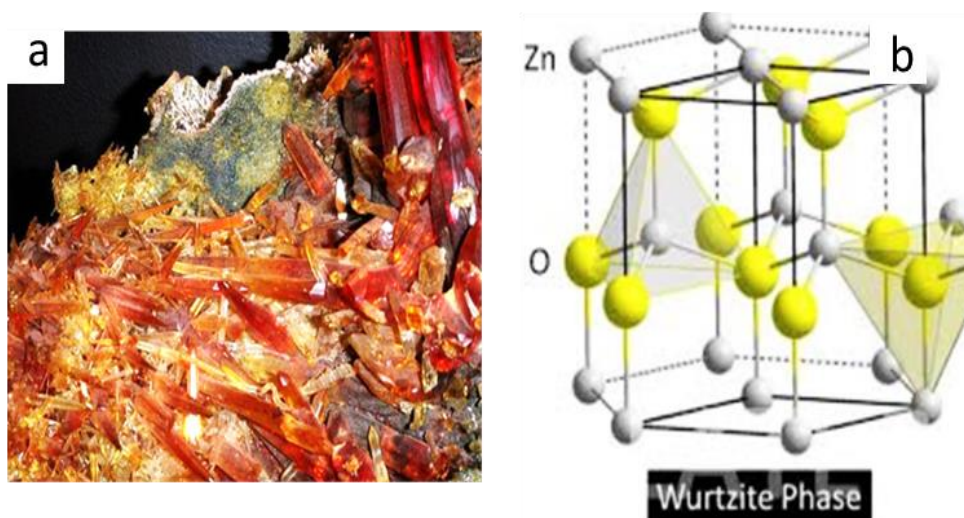


**Figure I.6.** (a) Photo of a zincite crystal (b) crystal structure of hexagonal wurtzite ZnO.

It is said that the stacking of the atomic planes of zinc (Zn) and the oxygen atom (O) of the Wurtzite structure are AaBbA type. The elementary mesh of the structure wurtzite is prismatic with a pattern of four atoms [24]:

-Two Zn atoms occupy the sites:  $(0, 0, 0)$  and  $(1/3, 2/3, 1/2)$ .

-Two O atoms occupy the sites:  $(0, 0, 3/8)$  and  $(1/3, 2/3, 7/8)$ .



**Table I.2.** Some characteristics and configuration of the mesh hexagonal ZnO.

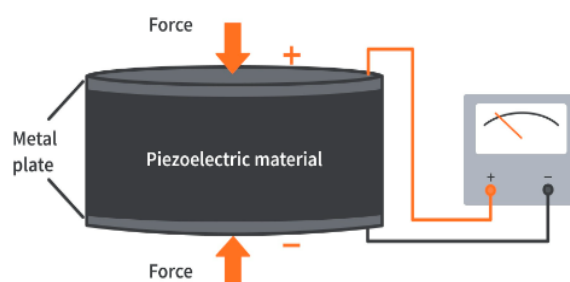
Structure type	Hexagonal Wurtzite
Mesh parameter	a=3.250 c=5.207 c/a=1.60
Distance between closest coordination's Tetrahedral O <sup>-2</sup> and Zn <sup>+2</sup> (Å)	Along the c axis: d=1.96 Following the other directions: d=1.98
Crystal ray for coordination tetrahedral (Å)	Zn :0.7                      O :1.24

### I.2.1.2. Piezoelectricity properties of ZnO

Piezoelectricity refers to the property possessed by certain bodies of electrically polarize either by generating an electric field or potential under the action of mechanical stress (Figure I.7). Zinc oxide belongs to the class of piezoelectric materials [24].

ZnO has been used as a piezoelectric material in various devices such as: mechanical probe, acoustic microscope, optical acoustic devices and SAW (surface acoustic wave) devices. The latter present an interesting application of thin films of ZnO, whose principle is based on the propagation of surface acoustic waves thanks to the variety of their use as filters and resonators for telecommunication systems, wireless sensors for remote measurement, the choice of ZnO in this field relates to the following properties [12,24,25]:

- a hexagonal crystalline structure which is part of the 6mm symmetric group the orientation of its c axis is said to be perpendicular to the substrate so that the piezoelectric effect can be used,
- high propagation speed of acoustic waves,
- a high electromechanical coupling coefficient  $K^2 = 7.3\%$ .

**Figure I.7.** Illustration of the behavior of a piezoelectric pellet.



### I.2.1.3. Optical properties of ZnO

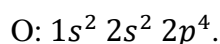
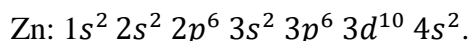
Zinc oxide is a transparent material in the visible range thanks to its very large optical gap that can vary from 3.1 to 3.4 eV (transparent in the visible and infrared range), its static refractive index in the bulk state is equal to the optical properties of ZnO in the form of a thin films vary according to the deposition conditions, its transparency can reach up to 90%. And large exciton binding energy of 60 meV [26]. The transmission, reflection, absorption are intrinsic properties of the film dependant on the chemical composition.

**Table I.3.** Some optical properties of ZnO.

Absorption coefficient ( $cm^{-1}$ )	$10^4$
Refractive index at 590 nm	2.013-2.029
Excitonic band width (meV)	60
Transmittance (%)	90

### I.2.1.4. Electrical Properties of ZnO

The electronic band structures of oxygen and zinc are:



The electrical conduction of zinc oxide is due to the presence of zinc atoms in interstitial sites as well as oxygen vacancies. On the other hand, the stoichiometric ZnO is an insulator. Doping improves the electrical conductivity of this material. The zinc oxide is a TCO that can have p-type or n-type doping [8].

Understanding the conduction behavior, due to two reasons. First,  $n$  and  $\mu$  cannot be independently increased for practical TCOs with relatively high carrier concentrations. At high electron density, carrier transport is limited primarily by ionized impurity scattering the Coulomb interactions between electrons and the dopants. Higher doping concentration reduces carrier mobility to a degree so that the conductivity cannot be increased [27].

### I.2.1.5. Catalytic and chemical properties of ZnO

Semiconductors such as ZnO are excellent reaction catalysts oxidation, dehydrogenation and desulfurization. The effectiveness of zinc oxide depends on how it is prepared. In water, it

can act as a catalyst photochemical for a number of reactions like the oxidation of oxygen to ozone, the oxidation of ammonia to nitrate, the reduction of methylene blue, the synthesis of hydrogen peroxide, or the oxidation of phenols [12,25].

### **I.2.2. ZnO applications**

Due to its semiconductor, piezoelectric, optical and catalytic properties, zinc oxide thin film has a variety of applications. It occupies an important place in the electronics industry. ZnO can be used as mechanical sensors or electronic devices such as rectifiers, Filters, resonators for radiocommunication and image processing [28]. Especially with the development of telecommunications, surveys have recently manufactured for use in surface acoustic wave devices, this due to their high electromechanical coupling coefficient [29].

### **I.2.3. Choice of dopants**

Zinc oxide is very interesting for various technological applications thanks to its different physico-chemical properties which make it interesting for compared to other oxides. Several researchers have studied the doping effect of diapers thin films of ZnO by different dopants. Indeed, ZnO can be doped with Co, In, Al, Mn, Ga, and Ni [30]. The choice of dopant is governed by the type of application sought.

ZnO thin films doped with copper made the object of in-depth studies because they present a high mobility, a transparency high optics and high electrical conductivity.

## **I.3. Copper oxides**

Copper has two oxidation states +1 and +2, and under special circumstances some trivalent compounds are also reported. It has been shown that this trivalent copper does not survive more than a few seconds. Therefore, cuprous oxide (Cu<sub>2</sub>O) and cupric oxide (CuO) are the two stable forms of copper oxide [31].

### **I.3.1. Cuprous oxide (Cu<sub>2</sub>O)**

Cu<sub>2</sub>O was the first known oxide semiconductor. Its semiconductor properties have been discovered in 1917 thanks to the work of Kennard. Cu<sub>2</sub>O never stopped attracting the interest of many researchers in several areas (Figure I.8), including photovoltaic cells since then It has been used for many years as a light absorber in solar cells [32].

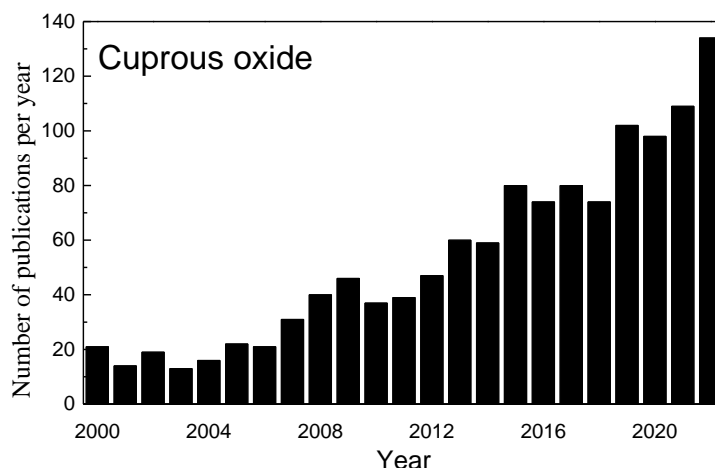


**Figure I.8.** Number of publications with the keyword of cuprous oxide in their title on the science direct website page from 2000 to 2022.

### I.3.1.2. Properties of cuprous oxide

#### a. Structure properties of cuprous oxide

Cuprous oxide (Cu<sub>2</sub>O), naturally has a phase stable copper-oxygen binary system which crystallizes in a simple cubic structure with a mesh parameter  $a = 4.2696 \text{ \AA}$  which can be broken down into two sub-networks (Figure I.10): a face-centered cubic lattice (FCC) formed by  $\text{Cu}^+$  cations and a body-centered cubic lattice (BCC) formed by  $\text{O}^{2-}$  anions. While each atom of oxygen is bonded to four atoms of copper [33].

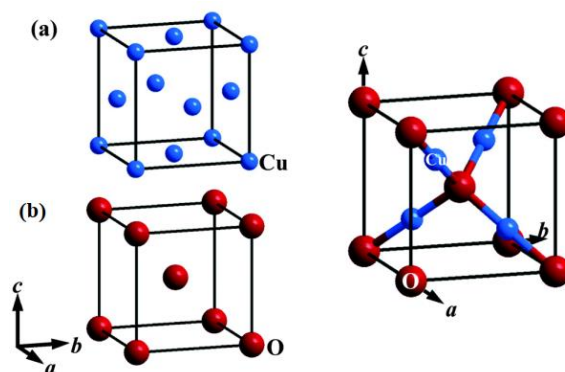


**Figure I.9.** The crystal structure of Cu<sub>2</sub>O, (a) face-centered cubic lattice of cations  $\text{Cu}^+$  and (b) centered-cubic lattice of anions  $\text{O}^{2-}$ .

#### b. Optical properties of cuprous oxide

Main theoretical calculations predict that Cu<sub>2</sub>O has a direct bandgap of about 1.97-2.1 eV, allowing the transmission of light of length wavelength greater than 580 nm (yellow range),

while that of lower wavelength at 580 nm is partially or totally absorbed. This is related to the fact that the band prohibited in thin films may vary depending on deposition conditions [34].

### c. Electrical properties of Cuprous oxide

Cuprous oxide is a p-type semiconductor with a wide mobility of positive charge carriers at ambient ( $\mu_p \sim 100 \text{ cm}^2 \cdot \text{V}^{-1} \cdot \text{cm}^{-1}$  in the form of a thin films) [35]. This mode of conduction has been attributed to the presence, at room temperature, of vacancies of copper [6].

## I.3.2. Cupric oxide (CuO)

### a. Structural properties of cupric oxide

The composition of cupric oxide has two phases: tetragonal and monoclinic. There tetragonal structure has lattice parameters ( $a=b=3.9 \text{ \AA}$  and  $c=5.3 \text{ \AA}$ ). CuO naturally stabilizes as monoclinic phase [36].

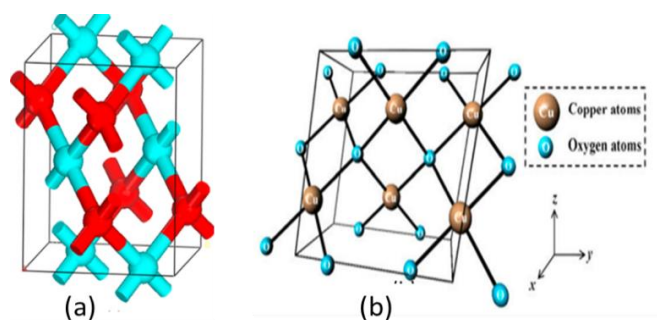


**Figure I.10.** Schematic representation of the crystallographic structure of CuO (a) tetragonal structure and (b) monoclinic structure [6].

### b. Electrical properties of cupric oxide

Cupric oxide is a p-type semiconductor with a narrow direct optical gap [35]. CuO generally has a low electrical conductivity ( $10^{-7} - 1 \Omega^{-1} \cdot \text{cm}^{-1}$ ), and this conductivity varies with the variation of the preparation method and also the deposition parameters [6].

### c. Optical properties of cupric oxide

CuO thin films color is black in appearance with a transmittance of 20% in the visible and could reach 90% for the high wavelength of the visible region [37]. The refractive index of CuO in the form of a thin film and its coefficient absorption vary according to the method elaboration and also according to the conditions of deposition [6].

## I.4. What are thin films?

In principle, a thin film is a layer of a material deposited on another material, called substrate, one the dimensions which we call the thickness has been greatly reduced so that this small distance between the two boundary surfaces remains the order of a  $\mu\text{m}$ , which gives the layer almost two-dimensional, which leads to a disruption the majority of physical properties. Very often such a small number of atomic layers has very different properties [33]. For example, optical reflection or absorption can be controlled in very precise ways, the same for the electrical conductivity [38].

### **I.5. Classification of growth patterns**

In a simple approach, the growth of thin films on a substrate is classified into three categories schematically illustrated (Figure I.11) [39,40].

#### **I.5.1. Island growth (Volmer-Weber mode)**

In this mode of growth, small clusters nucleate directly on the surface the substrate and grow in islands on it. This growth will take place when atoms or molecules that arrive on the surface of the substrate are more likely to bond between them than with the substrate. A typical case this growth is that metallic films on insulating substrates.

#### **I.5.2. Layered growth (Franck-Van der Merwe mode)**

This mode of growth takes place when the adatom-substrate interaction is very strong. The first atoms which arrive on the surface the substrate condense and form a monolayer covering the entire surface: we then have a growth two-dimensional of nuclei to form a layer, and then growth layer by layer.

#### **I.5.3. Mixed growth (Stranski-Krastanov mode)**

This mode of growth is an intermediate case: growth is first two-dimensional to form the first layer(s); however, as the energy of adatom-substrate interaction gradually decreases, the growth tends to become three-dimensional with the formation of islands.

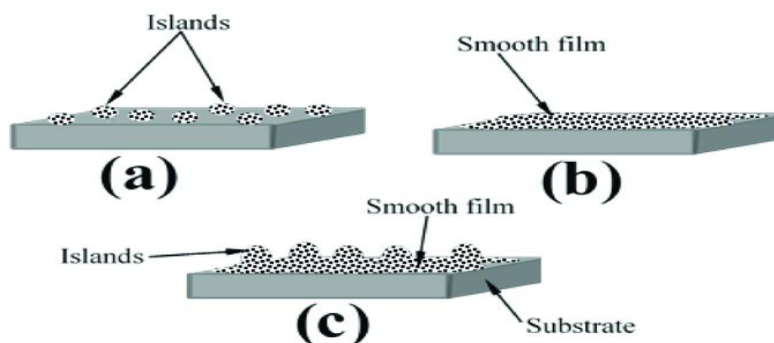


**Figure I.11.** Basic Modes of thin film growth: (a) island (b) layer-by-layer and (c) layer plus island.

### I.6. Thin films preparation Techniques

Generally, any thin film deposition follows the sequential steps: a source material is converted into the vapor form (atomic/molecular/ionic species) from the condensed phase (solid or liquid), which transported to the substrate and then it is allowed to condense on the substrate surface to form the solid film [41]. Depending on how the atoms/molecules/ions or clusters of species are created for the condensation process, the deposition techniques are broadly classified into two categories (Figure I.12): physical methods and chemical methods.

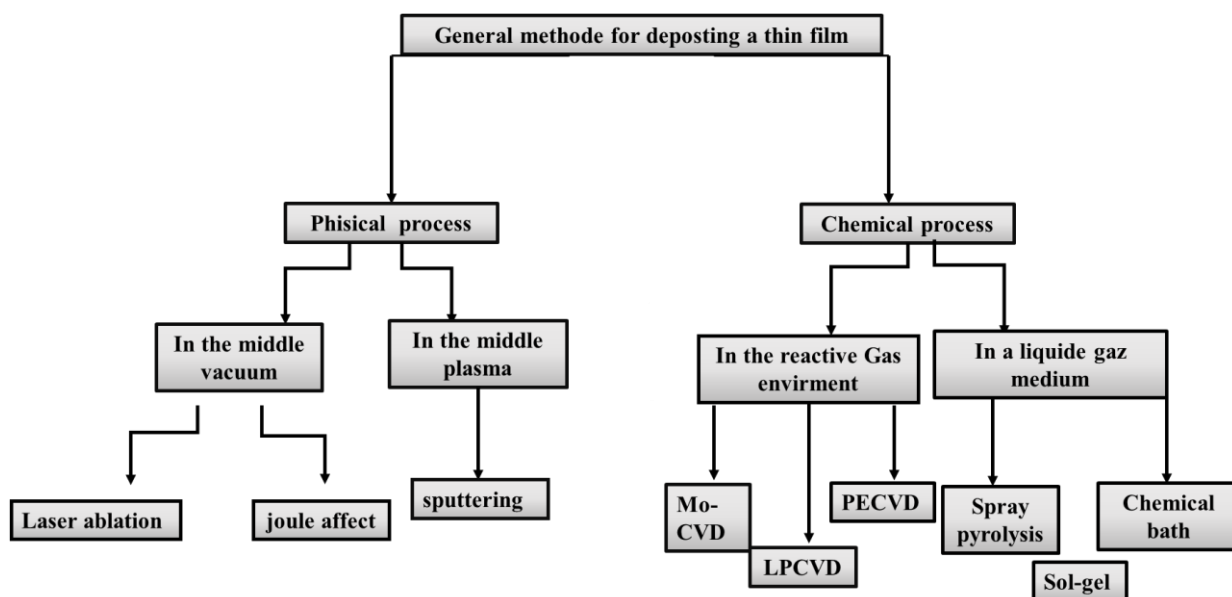


**Figure I.12.** Classification of thin film deposition techniques [1].

#### I.6.1. Physical process

PVD processes mainly include evaporation, laser ablation and sputtrng in all its forms. In the realization of a layer, we can distinguish the following three steps [42]:

- the creation of the species to be deposited, in the form of atoms, molecules or clusters (groups of atoms or molecules),
- the transport of these species in the vapor phase from the source to the substrate,
- the deposition on the substrate and the growth of the layer.

### I.6.1.1. In the vacuum middle

The vapors of the material to be deposited are obtained by heating it by different means: Joule effect, induction (coupling of a high frequency generator), cannon electrons, evaporation is carried out under a high vacuum (pressure of the order of  $10^{-3}$  to  $10^{-4}$ Pa) in order to increase its speed. As the vapor flow is localized and directional, it is often necessary to print at substrate a movement of rotation or translation relative the source of evaporation, so as to achieve a homogeneous deposit of uniform thickness. The best results are obtained on surfaces practically perpendicular to the vapor flow. When the pressure is not low enough the deposits are not very adherent and often amorphous [43].

#### a. Laser ablation method

With the Laser ablation or Pulsed Laser Deposition (PLD) method (Figure I.13), thin films are prepared by the ablation of one or more targets illuminated by a focused pulsed-laser beam. It is a physical vapor deposition process, carried out in a vacuum system, which shares some process characteristics common with molecular beam epitaxy and some with sputter deposition.

In laser ablation, each ablation pulse will typically provide material sufficient for the deposition of only a sub monolayer of the desired phase. The amount of film growth per laser pulse will depend on many experimental parameters, which have a strong influence on film properties. Laser related parameters such as laser fluence, including target–substrate separation; background gas pressure and laser spot size, and laser energy density. Under typical conditions, the deposition rate per laser pulse can range from 0.001 to 1Å per pulse [10].

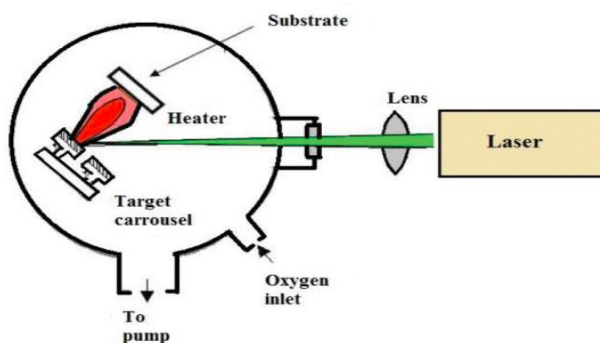
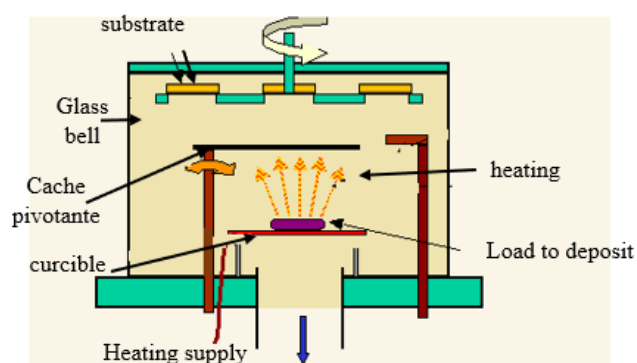


Figure I.13. The pulsed laser deposition (PLD) method [44].

### b. Joule effect method

The technique of thermal evaporation is strongly dependent on two parameters: thermally vaporized material and applying a potential difference to the substrate under medium or higher vacuum level ranging from  $10^{-5}$  to  $10^{-9}$  mbar [44], this type of evaporation consists in depositing the desired material evaporation by a filament, boat or crucible (Figure I.14), generally made from refractory metals (tungsten, tantalum, molybdenum, or alumina), the disadvantages of this technique are often sub-stoichiometric film development, low adhesion layers and the need for a fairly large power density to produce the phase gaseous materials with a very high melting point [44].



**Figure I.14.** Schematic of Joule effect technique.

#### I.6.1.2. In the plasma middle

Sputtering is one the most versatile techniques used for the deposition of transparent conductors when device quality films are required. Sputtering process produces films with better controlled composition, provides films with greater adhesion and homogeneity and permits better control of film thickness. The sputtering process involves the creation of gas plasma usually an inert gas such as argon by applying voltage between a cathode and anode. The target holder is used as cathode and the anode is the substrate holder. Source material is subjected to intense bombardment ions. By momentum transfer, particles are ejected from the surface of the cathode and they diffuse away from it, depositing a thin film onto a substrate. Sputtering is normally performed at a pressure of  $10^{-3} - 10^{-2}$  torr [2].

Normally, there are two modes of powering the sputtering system; DC and RF biasing. In DC sputtering system a direct voltage is applied between the cathode and the anode. This method is restricted for conducting materials only. RF sputtering is suitable for both conducting and non-conducting materials; a high frequency generator (13.56 MHz) is connected between the electrodes of the system. Magnetron sputtering is a process in which the sputtering source



uses magnetic field at the sputtering target surface. Magnetron sputtering is particularly useful when high deposition rates and low substrate temperatures are required [2].

## I.6.2. Chemical process

### I.6.2.1. Chemical vapor deposition

The Chemical Vapor Deposition (CVD) process, consists of causing chemical reactions between several gases or vapors to form a solid deposit on a heated substrate [10]. The temperature needed to cause the chemical reactions depends on the type of reactants used, and the type of desired reactions. This temperature is often very high, the most widely used CVD synthesis techniques are [22]:

- ❖ deposition by decomposition of organometallic compounds (MO-CVD). The metallo-organic precursors are components for which an atom of a element (Zn, Al, Ga, Si,...) is bonded to one or more carbon atoms of a organic hydrocarbon group. These precursors generally decompose at a low temperature, less than 500°C.
- ❖ Plasma-enhanced chemical vapor deposition (PE-CVD).
- ❖ Photo-CVD.
- ❖ And recently electrophoresis deposition for ZnO “nanowire” films.

The main advantages of these techniques are to allow the crystallization of films without resorting to annealing, to be able to control the composition during the deposition, to achieve a deposit of uniform thickness and composition with excellent adhesion. However, these techniques have the disadvantage of giving films contaminated by residues. Precursors and that of having an often-high reaction temperature [45].

### I.6.2.2. Chemical solution deposition

#### a. Sol–Gel Method

- **Sol:** a stable suspension of colloidal solid particles or polymers in a liquid.
- **Gel:** porous, three-dimensional, continuous solid network surrounding a continuous liquid phase.

Sol-gel is a chemical synthesis technique for preparing glasses, gels and ceramic powders. For the purposes of many theses, it will serve as an easy way to make high purity glass in solution form at room temperature. In the sol-gel process, a system of colloidal particles in a solution (sol) becomes a macroscopic material (gel), which is interpenetrated by a liquid [46].

There are different sol-gel methods:

**Dip Coating:** In a dip-coating process, a substrate is dipped into a liquid coating solution and then is dragged from the solution with controlling withdrawal speed as described in figure I.15. Generally, the thickness increases at faster dragging speed. The measurement of thickness by the equilibrium of forces at the stagnation point on the liquid surface [47]. The thickness is primarily affected by fluid viscosity fluid density, and surface tension. Therefore, a faster dragging speed pulls more fluid up onto the substrate before it has time to flow back down into the system, should be occur. While excellent for producing high- quality, uniform coatings, requires precise control and a clean environment. The applied coating may remain wet for several minutes until the solvent evaporates. This process can be accelerated by heated drying. Dip-coating technique is almost used to fabricate transparent layers of oxides on a transparent substrate with a high degree of planarity and surface quality [22].

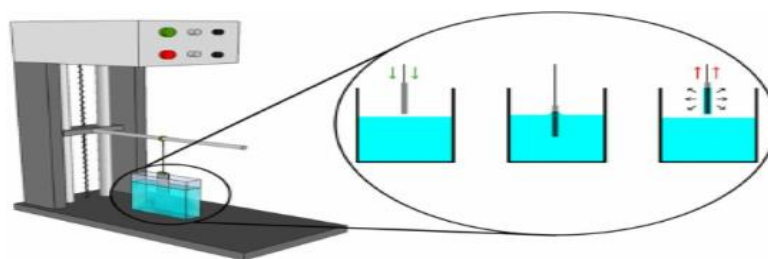


**Figure I.15.** Schematic model describing the film formation during the dip-coating process [22].

**Spin Coating:** The precursor is dropped onto the centre of a spinning substrate which then spreads out quickly and evaporates the solvent, see figure I.16. The Spin coating an exemplary process includes depositing a small puddle of a solution onto the center of a substrate and then spinning the substrate at high speed (typically around 3000 rpm) [48]. Centripetal acceleration will cause most of the resin to spread to, and eventually off, the edge of the substrate, leaving a thin film of material on the surface.

Final film thickness and other properties will depend on the nature of the fluid material (viscosity, drying rate, percent solids, surface tension, etc.) and the parameters chosen for the spin process. Factors such as final rotation speed, acceleration, and fume exhaust affect the properties of the coated films. One of the most important factors in spin coating is repeatability, as subtle variations in the parameters that define a spin-coating process can result in drastic variations in the coated film [22].

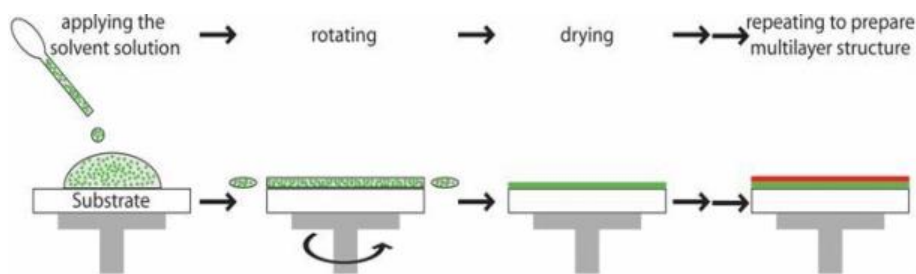


**Figure I.16.** Schematic model describing the film formation during the spin-coating process [22].

### b. Chemical bath deposition method

The chemical deposition of films on a solid substrate is due to reactions which produce in an aqueous solution (chemical bath). So, CBD is a technique in which thin films are deposited on substrates immersed in solutions diluted containing metal ions and a source of chalcogenide [49,50]. In the chemical bath deposition procedure, the substrate is immersed in a solution containing the precursor. This method depends upon parameters such as bath temperature, pH of the solution, the molarity, and time. Figure I.17 represents the simple chemical bath deposition method [44].

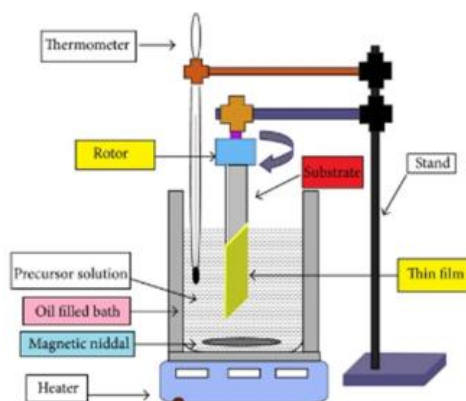


**Figure I.17.** Chemical bath deposition technique.

### c. Spray pyrolysis method

The Spray pyrolysis technique is a chemical deposition process being used in research to prepare thin and thick layers. Unlike in many other coating techniques, the spray technique represents a very simple and relatively cost-effective processing method (particularly in terms of relates to equipment costs). It offers an extremely easy technique for preparing films of any composition [45]. This technique consists in projecting a solution containing the elements that we want to deposit on a heated substrate, all under a controlled atmosphere. For the synthesis of oxide films. The advantage of such a method is its simplicity and low material cost as well as good control of the deposition conditions (temperature of the substrate, concentration of the starting solution, etc.) [51].

There are Two methods are generally used to spray the solution containing the source material:

- **Pneumatic spraying:** The production of the fog is carried out by a compressed gas which sucks and bursts the liquid (Figure I.18.a) [52,53].
- **Ultrasonic spray pyrolysis:** The aerosol is generated from the high frequency vibrations produced within the solution, and localized towards the free surface of the liquid (Figure I.18.b).

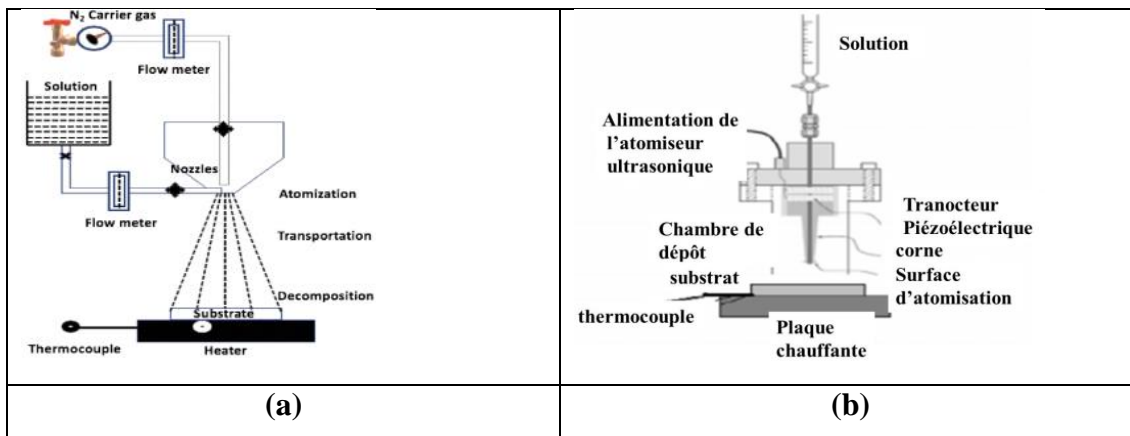


Figure I.18. Spray pyrolysis method using; (a): Pneumatic, (b): Ultrasonic.



# Chapter II

Elaboration of ZnO:Cu thin films and analysis  
technique



## Chapter II. Elaboration of copper-doped zinc oxide thin films and analysis techniques

This chapter will be introduced apply of undoped and copper-doped zinc oxide thin films by ultrasonic spray pyrolysis technique was used for this deposition and then we move on to optical characterization methods (UV-Vis-NIR spectroscopy) and electrical characterization (four probe technique) of the samples.

### Part one: Elaboration copper-doped zinc oxide thin films

#### II.1. Ultrasonic spray pyrolysis

Ultrasonic spray pyrolysis is a technique that requires a precursor solution, for example  $\text{Zn}(\text{CH}_3\text{COO})_2$  and  $\text{CuCl}_2$  in the form as solution used in the study and a heated substrate and atomizer. The solution is sprayed, in fine drops by a 40 KHz ultrasonic generator. It allows the transformation of the solution to the nozzle level into a jet of very fine droplets  $\sim 40\mu\text{m}$  in diameter [6]. The jet arrives on the surface of the substrates which are heated which allows the activation of the chemical reaction. In the appropriate experimental conditions, the vapor formed around the droplet prevents the direct contact between the liquid phase and the surface of the substrate. This evaporation of droplets allows a continuous renewal of the vapour, therefore the droplets undergo the thermal decomposition and lead to the formation of strongly adherent films [54].

##### II.1.1. Stages of forming thin films by spray pyrolysis technique

In spray pyrolysis, precursor solution is atomized through a nozzle. The nozzle converts the solution into small droplets, known as aerosols. These aerosols are allowed to incident onto the heated substrates. The paralytic decomposition of the aerosols depends on substrate temperature. The formations of thin films with desired properties are possible only at optimum substrate temperature. Various steps during paralytic decomposition of aerosols are summarized as [55].

1. In the first step, an aqueous precursor solution is converted into aerosols by ultrasonic waves at the atomizer nozzle,
2. Solvent evaporation takes place in the second step,
3. In this step, vaporization of the solvent leads to precipitate formation as the droplets / aerosol approaches the substrate,

4. In next step, when the precipitate reaches the substrate, nucleation and growth of metal oxide thin films,

5. Finally, growth of the nuclei leads to the formation of continuous thin layer of metal oxide.

### II.1.2. What are the advantages of spray pyrolysis?

The spray pyrolysis technique has received great interest from researchers and scientists due to several advantages [6,44,56,57]:

- The thin film that is produced is in a steady state,
- The spray pyrolysis technique allows for the natural growth of the sample,
- The ability to control the shape of thin films,
- Obtain a homogeneous film,
- Cheaper and less expensive,
- Spray pyrolysis is a fast process,
- Several products can be used at the same time, in particular for doping.

### II.1.3. Factors affecting thin film preparation by ultrasonic spray pyrolysis technique

The principle of thin film formation by ultrasonic spray pyrolysis method depends on:

#### II.1.3.1. Atomization rate and droplet size

The size of the droplet is an important factor. If it is very large, the heat is not sufficient to convert it into vapor, and this leads to the formation of a solid, heterogeneous precipitate. If the drop is very small, then the drop dries before it reaches the substrate. This means that the solvent evaporates and the rest of the substance, so we notice black dots on the substrate indicating the burning of the substance, but if the drop size is medium, which is the ideal condition for precipitation, as it evaporates the solvent is a little before reaching the substrate, so it reaches the substrate in the form of vapor, and thus the reaction takes place on the base and the formation of the film [57].

#### II.1.3.2. Effect of substrate temperature

The most important factor in the formation of thin films is the temperature where (Figure II.1) [58]:

- If the temperature is low, do not allow thin films to form.
- If the temperature is high, the solution will evaporate before it reaches the substrate.



- At a suitable temperature, the solution is deposited on the substrate, a homogeneous and crystalline thin film is formed.

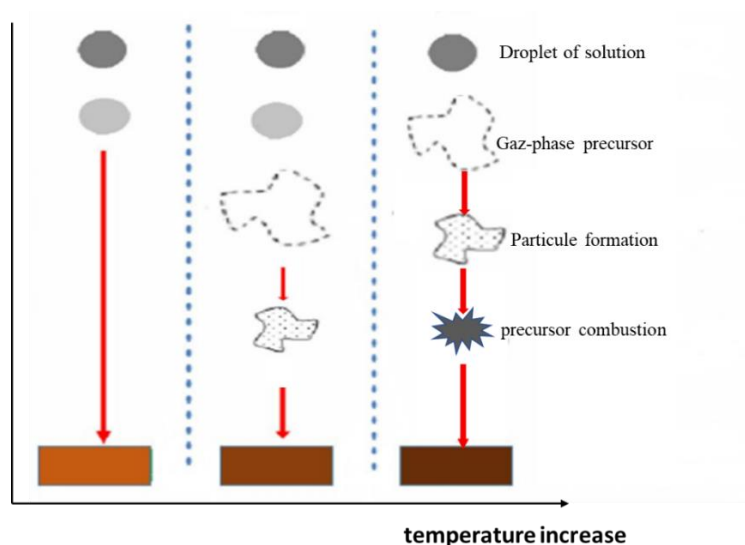


**Figure II.1.** Effect of substrate temperature on the formation of thin films [51].

### II.1.3.3. Effect of deposit time

The time period for sedimentation of thin films must be considered because if the time period during spraying is long, then the film formed is thicker [59], but if the period is short, then the film formed is very thin, meaning that its atoms are not compact.

### II.1.3.4. Effect of the nozzle-substrate distance

In fact, at a small distance from the nozzle to the substrate ( $D_1$ ), spraying the solution containing the various precursors causes droplets to flow at a high density so that the solution does not pass through the vapor phase and remains in the form of a liquid that hinders the formation of a layer on the substrate.

For a relatively long distance ( $D_3$ ), the droplets formed following the spraying the solution that contains our various precursors produce a sort of powdery matter found on the substrate, and this because of the fairly long journey that these droplets set to get to the surface of the substrate.

The nozzle-substrate distance ( $D_2$ ) gave good deposits (Figure II.2), which are well adhered to the surface of the substrate because the appropriate distance helps the solution to pass through the stages in order, solution, then vapor evaporation of the solvent and the survival of the



material to be deposited, then the adhesion of the material to the substrate and the formation of the thin film [60].

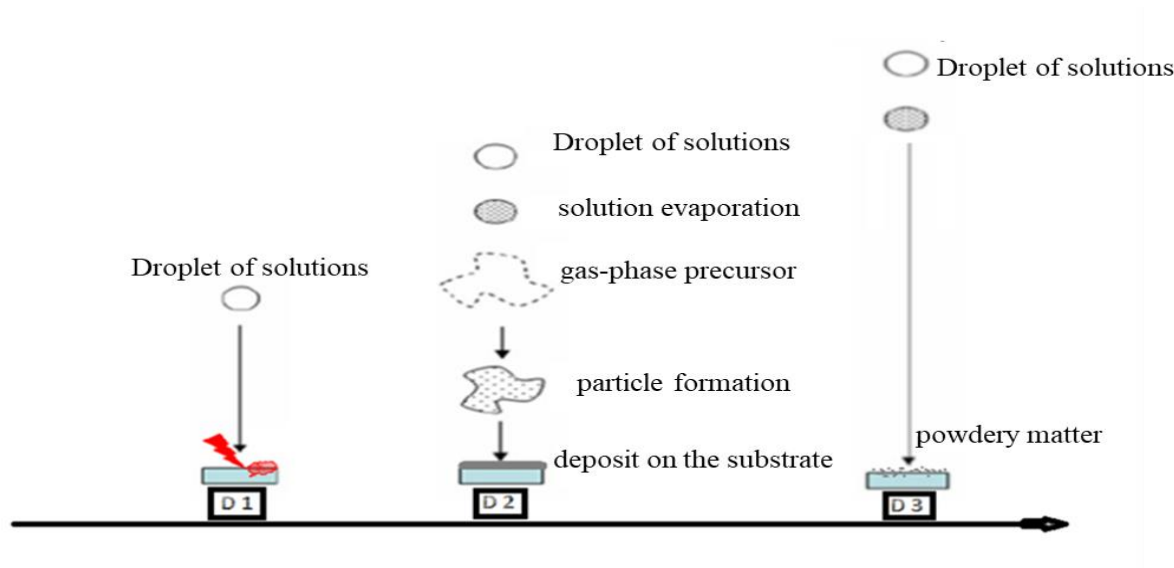


**Figure II.2.** Effect of Nozzle-substrate distance on film elaboration [60].

## II.2. Experimental procedure

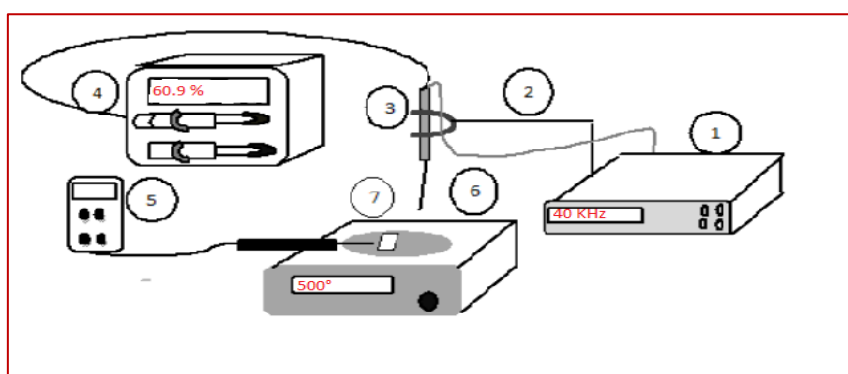
The objective of this work is the production of undoped zinc oxide (ZnO) and copper-doped zinc oxide (ZnO:Cu) thin films by the ultrasonic spray pyrolysis technique at two different distances between the nozzle and the substrate ( $d_{N-S}$ ) with fixing all the other experimental parameters (deposition temperature ( $T_D$ ), solution concentration ( $C$ ), deposition time ( $t_D$ ), solution flow rate( $\phi$ )), and the study of the effect of copper doping and nozzle-substrate distance on the optical and electrical properties of zinc oxide samples. The precursor solutions used are zinc acetate dihydrate ( $Zn(CH_3COO)_2 \cdot 2H_2O$ ) and copper chloride dihydrate ( $CuCl_2 \cdot 2H_2O$ ) in distilled water as a solvent.

## II.3. Followed equipment

The experiment was carried out at the level of Laboratory of Materials and Structure of Electromechanical Systems and their Reliability (LMSSEF: *Laboratoire des matériaux et structure des systèmes électromécaniques et leur fiabilité*) of Larbi Ben M'hidi University of Oum El Bouaghi, it was prepared the undoped and copper-doped zinc oxide thin films by ultrasonic spray pyrolysis technique from the simple elements (Figure II.3 and Figure II.4).



**Figure II.3.** Equipment used in ultrasonic spray pyrolysis technique.



1. Ultrasonic generator
2. Support
3. Nozzle
4. Syringe pump
5. Digital thermometer
6. heating plate
7. Glass substrate

**Figure II.4.** Schematize Ultrasonic Spray Pyrolysis (USP) [61].

-processing components:

- 1. Ultrasonic generator:** allows decomposing the solution at the atomiser to very fine droplet.
- 2. Support**
- 3. Nozzle:** contains a nozzle from which the solution comes out in the form of vapor.
- 4. Syringe pump:** model PHOENIXD-CD(GF-FOURES) to control the precursor solution flow rate.
- 5. Digital thermometer:** it is a device to measure the temperature. In this work, thermocouple tip (type K/NiCr-NiAl) is connected to the heater.
- 6. Heating plat:** Its task to heat the substrate.
- 7. Glass substrate:** film is deposited.

## II.4. Stages of preparation thin films

### II.4.1. Choice the substrate

The choice of the substrate is an important matter in the process of manufacturing thin films, and this is in order to ensure the safety of the films and its excellent growth. Therefore, glass was chosen as a substrate because of its favorable adhesion force that allows the placement of the thin film on the substrate in addition to its compatibility with the coefficient of thermal expansion [24]. The glass has expansion coefficient similar to that of zinc oxide and copper oxide, in order to avoid pressure on the substrate ( $\alpha_{glass} = 8.5 \times 10^{-6} K^{-1}$ ,  $\alpha_{ZnO} = 7.2 \times 10^{-6} K^{-1}$ ,  $\alpha_{CuO_2} = 2.5 \times 10^{-6} K^{-1}$ ), in addition to the economic reasons and the transparent property [10,51].

### II.4.2. Preparation the substrate



**Figure II.5.** Description cleaning process of the substrate.

The substrates that were used to deposit the films are glass microscope slides ( $2.45 \times 7.62$ )  $cm^2$  and 1 mm thick, each slide was cut into three substrates using a diamond

tip pen. Then substrates are cleaned to ensure that the films grow without impurities. Which go through several stages (figure II.5):

- ✓ The glass slides are cleaned using distilled water.
- ✓ Rinse with acetone bath.
- ✓ Cleaning with distilled water to avoid remaining traces of acetone.
- ✓ Soaking in ethanol to remove the lipid layer.
- ✓ Cleaning with distilled water to avoid remaining traces of ethanol (Figure II.5.a).
- ✓ Finally, using Joseph paper to dry substrates (Figure II.5.b).

➔ Glass slides were ultrasonically cleaned in each bath for approximately five minutes (Figure II.5.c and Figure II.5.d).

### II.4.3. Preparation of deposition solution

#### II.4.3.1. Preparation the solution of zinc acetate dihydrate

In this work, zinc acetate dihydrate (ZAD) of a molar mass  $M_{ZAD} = 219.49 \text{ g/mol}$  is used as a zinc source which has a white color (Figure II.6.a).

To obtain a solution of zinc acetate dihydrate, a mass ( $m_{ZAD} = C \cdot M_{ZAD} \cdot V$ ) of zinc acetate dihydrate powder (weighed with a balance) is dissolved in a volume V of distilled water (Figure II.6.b).



**Figure II.6.** Zinc acetate dihydrate as powder (a) and as solution (b).

#### II.4.3.2. Preparation the solution of copper chloride dihydrate

In order to use copper as a source of doping. From copper chloride dihydrate of molar mass  $M_{CCD} = 170.48 \text{ g/mol}$  which has a turquoise color in distilled water as a solvent. To obtain a solution of molarity ( $C=0.05 \text{ mol/l}$ ), a quantity ( $m_{CCD}=C \cdot M_{CCD} \cdot V$ ) in a volume V of distilled water (Figure II.7 and II.8).

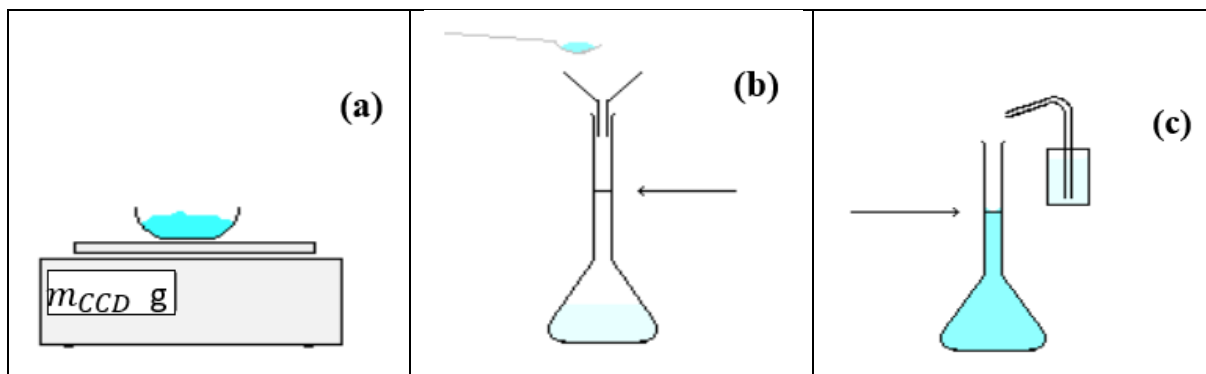


Figure II.7. Stage of preparation of copper chloride dihydrate solution.



Figure II.8. Copper chloride dihydrate as powder (a) and as solution (b).

#### II.4.3.3. Preparation the solution of precursor

After preparing each of the zinc acetate dihydrate solution and the copper chloride dihydrate solution, the two solutions are combined in a Becher of capacity 25ml. where is the volume of the acetate solution:  $V_{ZAD} = (1 - d) \times 25 / d$ : doping rate

$$V_{CCD} = d \times 25$$

Condition  $\longrightarrow V_{ZAD} + V_{CCD} = 25ml$

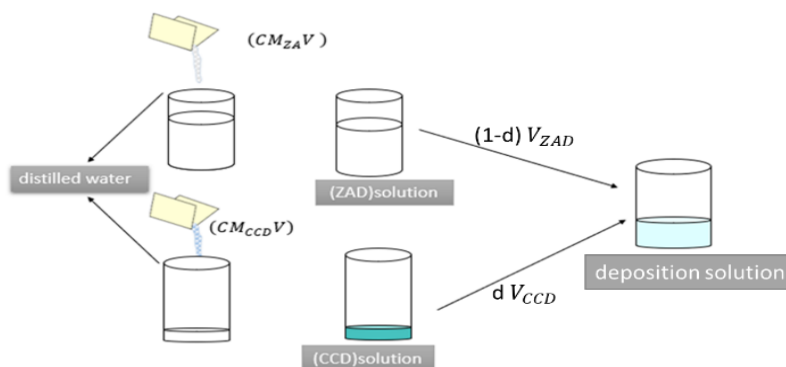


Figure II.9. Preparation the precursor solution.

#### II.4.4. Thin films preparation

To prepare the thin films that are under study, we follow the following steps:

- The first, step we take to ensure the proper functioning of thin film growth is to prepare all devices and ensure their safety,
- We placed the substrate above an electrical resistor, the substrate is gradually heated from room temperature up to the deposition temperature ( $T_s=300^\circ\text{C}$ ) in order to avoid thermal shock of the substrates,
- When heating is done, the precursor solution is placed in the syringe and the latter placed in syringe pump device, we install the flow rate where it is 60 ml / h, to ensure the solution flows slowly. By means of the Ultrasonic generator, the solution is broken up into small droplets close to the vapor,
- Finally, the deposition process takes place by spraying the solution on the hot substrate for 3 minutes. After which, the heating is stopped and the substrates are left to cool. To room temperature to avoid thermal shock that risks sample cracking, then our samples were recovered. We note that the deposited films were transparent and well adhered to the glass substrates.

#### Part two: Characterization techniques of thin films

After the process of preparing thin films, the latter is studied in terms of optical and electrical properties in order to obtain many information about the prepared sample.

#### II.1. Optical characterization of thin films

There are different ways to characterize thin films of transparent conductive oxides, UV- Vis spectrophotometer is among the optical method which helps to know many optical properties (band gap, absorption coefficient, particle size, thickness,...etc), which is obtained by studying the optical transmittance spectrum curve Figure II.10.b.

UV-Vis spectroscopy refers to the transmittance spectrum or reflection spectrum in the ultraviolet-visible spectral range. Transmittance or reflection of visible light has a direct effect on perceived content. Which measures the intensity of light passing through the sample  $I$  and compare it to the light intensity before passing the reference  $I_0$ . Ratio  $I/I_0$  is called light transmittance, usually expressed in percentage (T%) [62].

This spectroscopy involves electromagnetic radiation of energy noticeably high. The useful wavelength range in the devices is : Ultraviolet:  $300 \leq \lambda < 375$  nm and Visible-



NIR:  $375 \leq \lambda \leq 1100 \text{ nm}$ . This characterization technique is shown in the figure (II.10.a), it consists in measuring the intensity ( $I$ ) transmitted through the thin film for a whole range of wavelengths. Several spectral lamps emitting in UV, the visible and the near IR are placed successively at the entrance of a monochromator whose purpose is to select a wave length. The output of the monochromator, the sample is illuminated by this wavelength and  $I(\lambda)$  is measured after the sample (glass + layer) [24].

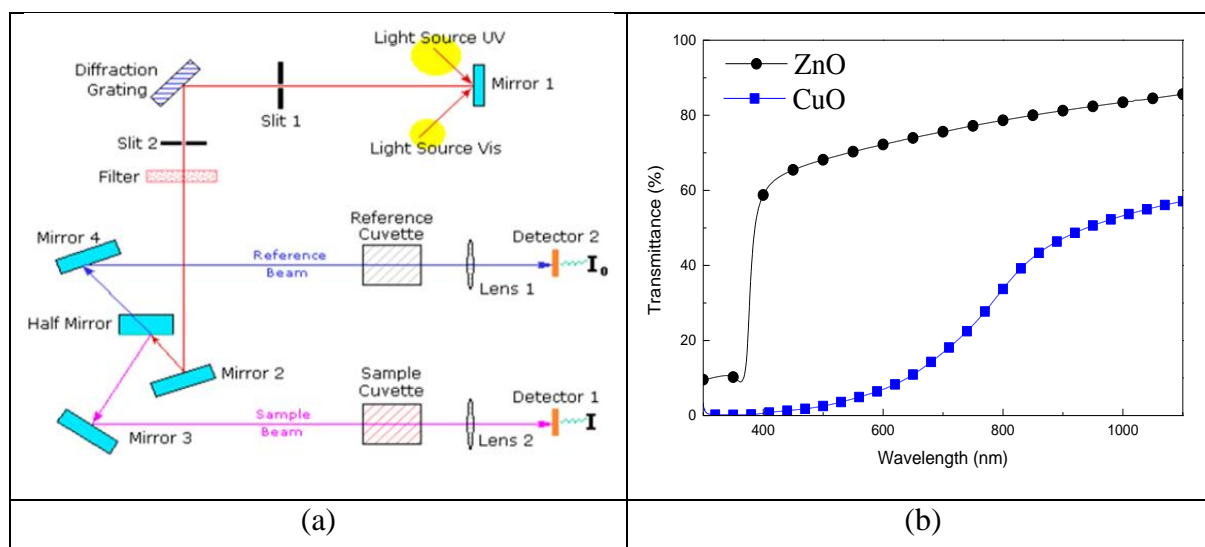


**Figure II.10.** (a) Principle of measure the transmission UV-Vis [24]  
(b)transmission spectrum example of copper oxide and zinc oxide thin films.

### II.1.1. Determination of film thickness and refractive index

The thickness and refractive index of film can be determined through the transparency curve, which can be divided into two fields, each field has a function related to the wavelength, and it has several constants, including thickness and refractive index, and using the least squares method, the best fit for the data; evidence using simple calculus and linear algebra, the basic problem is to find the graph  $y=f(x)$  provided that for  $n \in \{1, \dots, N\}$ , the pair  $(x_n, y_n)$  is observed. Least squares regression for prediction behavior of the dependent variable. We determine the thickness and refractive index of the copper-doped zinc oxide films from transmission spectra, using the Fit software allows changing number of parameters. We use least squares to adjust the simulated transmission curve to measured [11].

### II.1.2. Determination of absorption coefficient and optical band gap

The term “bandgap” refers to the energy difference between the peaks of the valence band at the bottom of the conduction band, electrons can jump from one band to another. For

Electrons need to go through a certain process to jump from the valence band to the conduction band. The minimum energy of the transition, the bandgap energy.

In order to calculate the energy gap, the absorption coefficient ( $\alpha$ ) must be passed through the application of the relationship [63]:

$$\alpha = \frac{1}{d} \ln \left( \frac{100}{T} \right) \quad (\text{II.1})$$

d: The thickness of the thin film.

T: transparency percentage (%)

The transmittance can be calculated by applying the Beer-Lambert [64]:

$$T = e^{-\alpha d} \quad (\text{II.2})$$

After the absorption coefficient has been calculated, the energy gap is determined from the diagram represented the relationship [20,65,66]:

$$(\alpha h\nu)^n = A(h\nu - E_g) \quad (\text{II.3})$$

$h\nu$ : Energy of incident photon (eV).

$E_g$ : Energy of the optical gap (eV).

A: Constant dependent on electron-hole mobility.

n: is an indicator that expresses the type of transmission [53]:

- ❖ If it is equal to 2, then it is a direct transmission
- ❖ If it is equal to 1/2, then it is not direct transmission

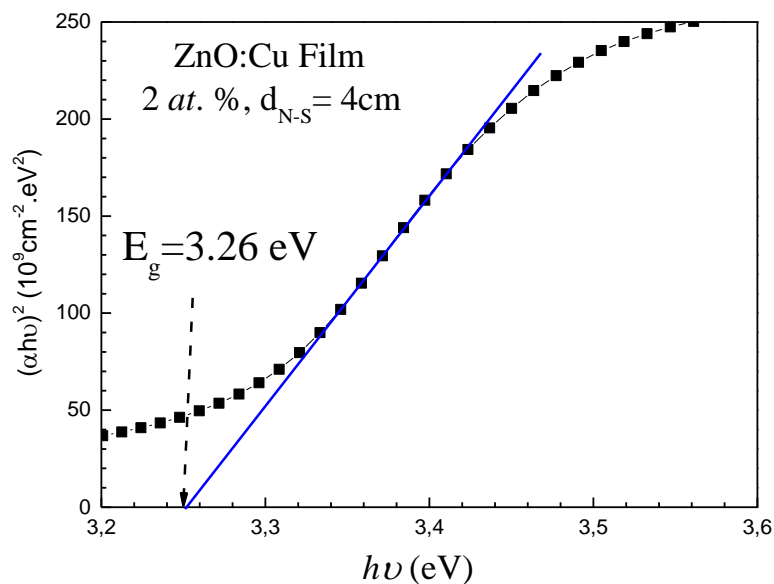


Figure II.11. Explanation of band gap.



### II.1.3. Determination of Urbach Energy

One of the most important elements in the study of optical properties is the Urbach energy, which helps the researcher to know many information about the prepared sample, for example knowing the stability of the sample. It is calculated by the expression shown [67]:

$$\alpha = \alpha_0 \exp \frac{h\nu}{E_{Urb}} \quad (\text{II.4})$$

$E_{Urb}$ : Energy of Urbach.

$\alpha_0$  : constant.

The curve  $\ln(\alpha) = f(h\nu)$  is plotted (Figure II.12), which is determined from the equation [30]:

$$\ln \alpha = \ln \alpha_0 + \frac{h\nu}{E_{Urb}} \quad (\text{II.5})$$

The Urbach energy is determined from the reciprocal of the slope.

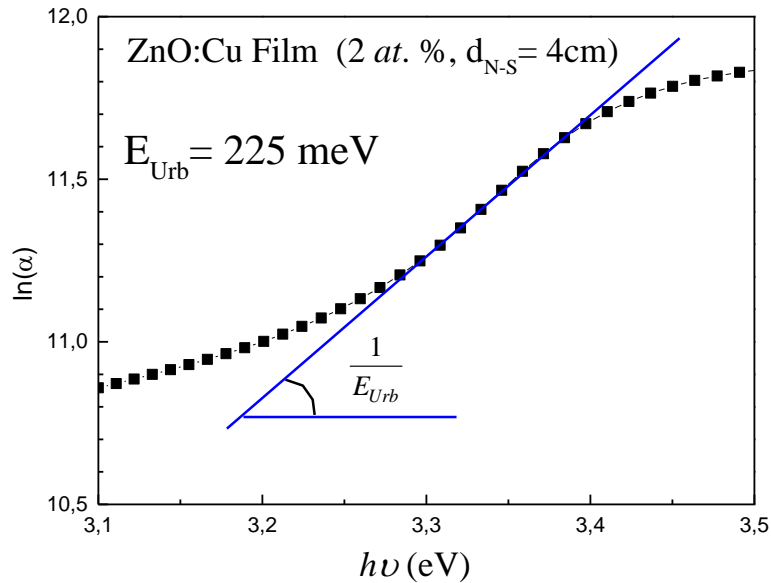
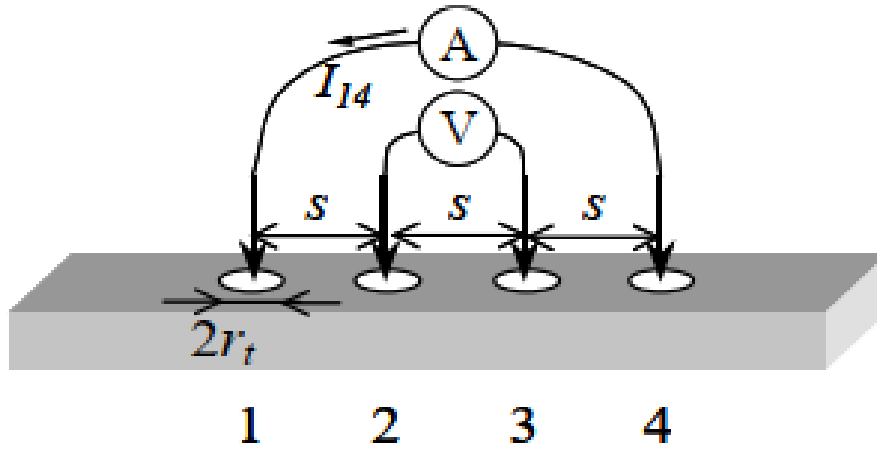


Figure II.12. Determination of Urbach energy.

## II.2. Electrical characterization of thin films

The electrical properties of the prepared thin films are studied by applying the four-point technique. The principle of this characterization technique is based on the application of a probe composed of four tungsten metal tips, aligned and equidistant (S) on the sample surface. The two outer electrodes bring the current  $I$  generated by a current source into the layer to be

analyzed, and the two inner electrodes serve to collect potential (V) induced by layer resistance (Figure II.13).



**Figure II.13.** Diagram representing the principle of the four-point method [11].

Since each pair of the four pins was equidistant during the measurement, and the thickness of the layer is much smaller than its lateral dimension as well as the distance between the pins, the sheet resistance ( $\rho_s$ ) can be calculated as follows [62,66]:

$$\rho_s = \frac{\pi V}{\ln 2 I} \quad (\text{II.6})$$

Therefore, the electrical conductivity ( $\sigma$ ) is related to the film thickness ( $d$ ) by the expression following [10,11]:

$$\sigma = \frac{1}{\rho_s \cdot d} \quad (\text{II.7})$$

In order to know electrical conductivity ( $\sigma$ ) of copper-doped zinc oxide thin films, we used Jandel four-point probe device was used in the LMSSEF laboratory of Larbi Ben M'hidi University at Oum El Bouaghi (Figure II.14), the probe consists of four contacts aligned linearly and the distance between the four terminals ( $S=1$  mm). A variable current ( $I$ ) is applied between the two external terminals and the voltage ( $V$ ) is measured between the two internal probes using Keithley 2400, which makes it possible to measure low voltages.



Figure II.14. Four-point device.



# Chapter III

## Results and discussion



### Chapter III: Results and discussion

The purpose of this chapter is to present and explain the experimental results of our work on the development and characterization of Cu-doped ZnO films deposited on glass substrates by ultrasonic spray pyrolysis technique, where the effect of copper doping rate on ZnO films is studied, in addition to studying the effect of the distance between the nozzle and the substrate on the optical and electrical properties. With constant conditions of deposition (deposition temperature ( $T_D$ ), solution concentration (C), deposition time ( $t_D$ ), solution flow rate ( $\phi$ )).

This study is done by UV-Vis-NIR spectrophotometer determination of basic optical properties (optical gap, Urbach energy and refractive index) and the average thickness of each deposited films. To determine the electrical properties, we used the four-probe method to determine our electrical conductivity samples.

#### III.1. Photos of our samples

Figure III.1 shows photographs of copper-doped zinc oxide (ZnO:Cu) samples deposited on glass substrates with different doping levels (0, 2, 4, 6, and 8 *at. %*) at two different distances. It was found that all the obtained samples are not very transparent compared to glass, as they differ in color according to the doping rate and the nozzle-substrate distance, so we notice that the sample is deposited at the far distance are more transparent than the sample deposited at close distance, with a special case at distance 6 cm it is very transparent when doping with 4 *at. %*, due to the experimental conditions.

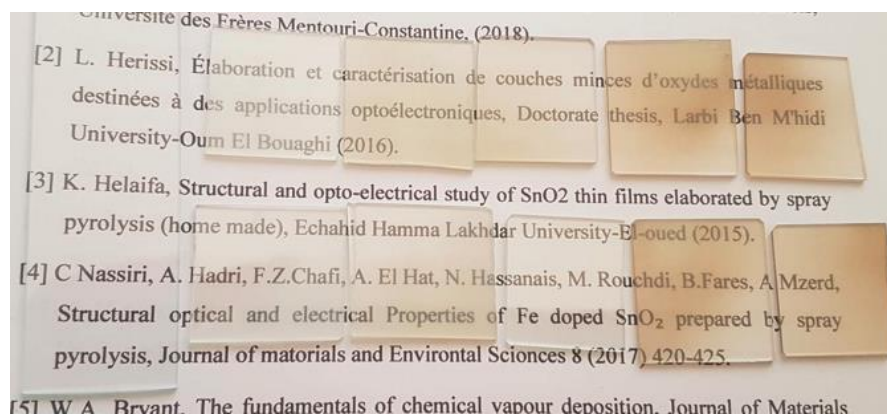


**Figure III.1.** Photos of thin films deposited on glass substrates.

Figure III.2 shows variation the luminosity of sample as a function of Cu concentration, we note decreases the luminosity as the percentage of the doping increase for the distance  $d_{N-S} = 4$  cm and  $d_{N-S} = 6$  cm, this is prove the darkness of the samples specially for

$d_{N-S} = 6$  cm, while for the distance  $d_{N-S} = 4$  cm when doped with 4 at % the sample was very luminous and this is was due to transparency the sample.

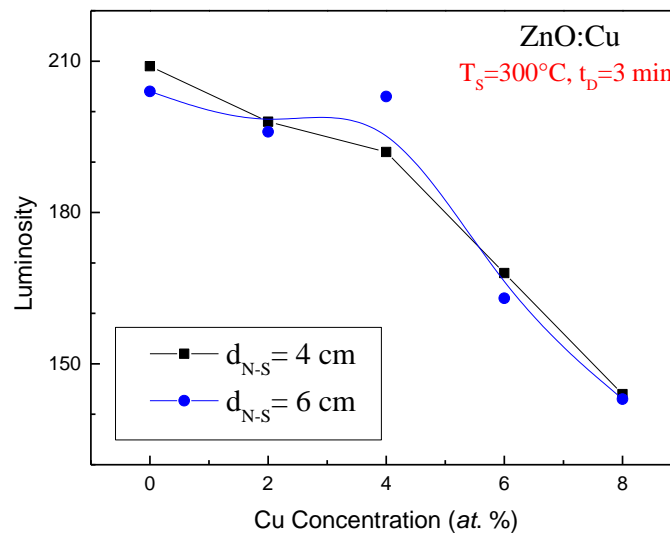


**Figure III.2.** Variation the luminosity of the samples with different Cu concentration

### III.2. Effect the doping with Cu and the distance on the thickness of ZnO thin films

The average thickness ( $d$ ) of copper-doped zinc oxide films was determined from an adjustment model based on the Swanepoel method which gives very convergent values which made it possible to deduce a certain number of optical parameters such as: the thickness ( $d$ ) and the optical indices ( $n$ , and  $k$ ) [68].

Figure III.3 represent the variation of average thickness of ZnO:Cu thin films as a function of the different doping percentages (at. %) prepared at two different nozzle-substrate distances.

Many authors have found that when doping is added as the films grow, their thickness increases regardless of the deposition technique or the nature of the doping [11], and this is what we found in our work. The thickness of the films increases gradually when the copper concentration is increased from 270 nm to 350 nm and from 240 nm to 330 nm at the preparation distance 4 cm and 6 cm, respectively. This increase can be interpreted by the increase in porosity in the deposited material, since it is well known that the variation in thickness is directly proportional to the porosity [23].

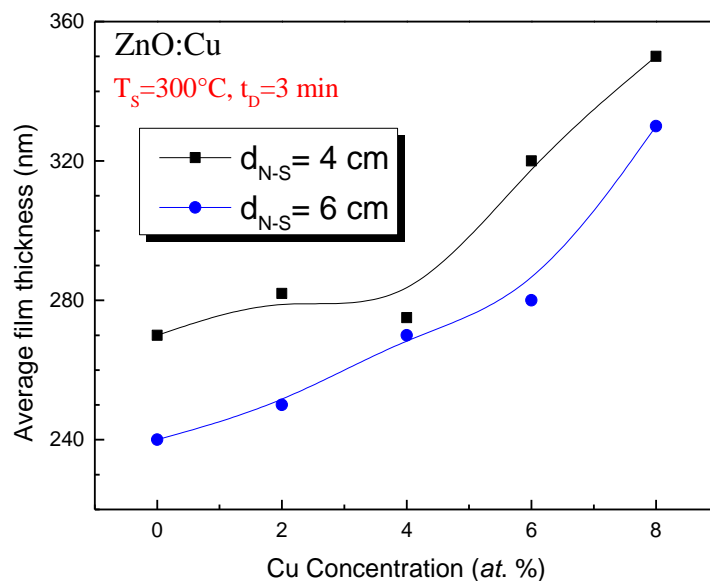


**Figure III.3.** Variation of average film thickness of ZnO as a function Cu concentration at two different distances.

Concerning the observed difference the thickness values between  $d_{N-S} = 4$  cm and  $d_{N-S} = 6$  cm. The samples prepared at close distances are thicker due the increase in the amounts of deposited materials (there are more materials that contribute to the formation of the membrane) [10]. In contrast to the samples that were prepared at far distances because the required main substance amount concentration (Cu and Zn) failed to reach the substrate.

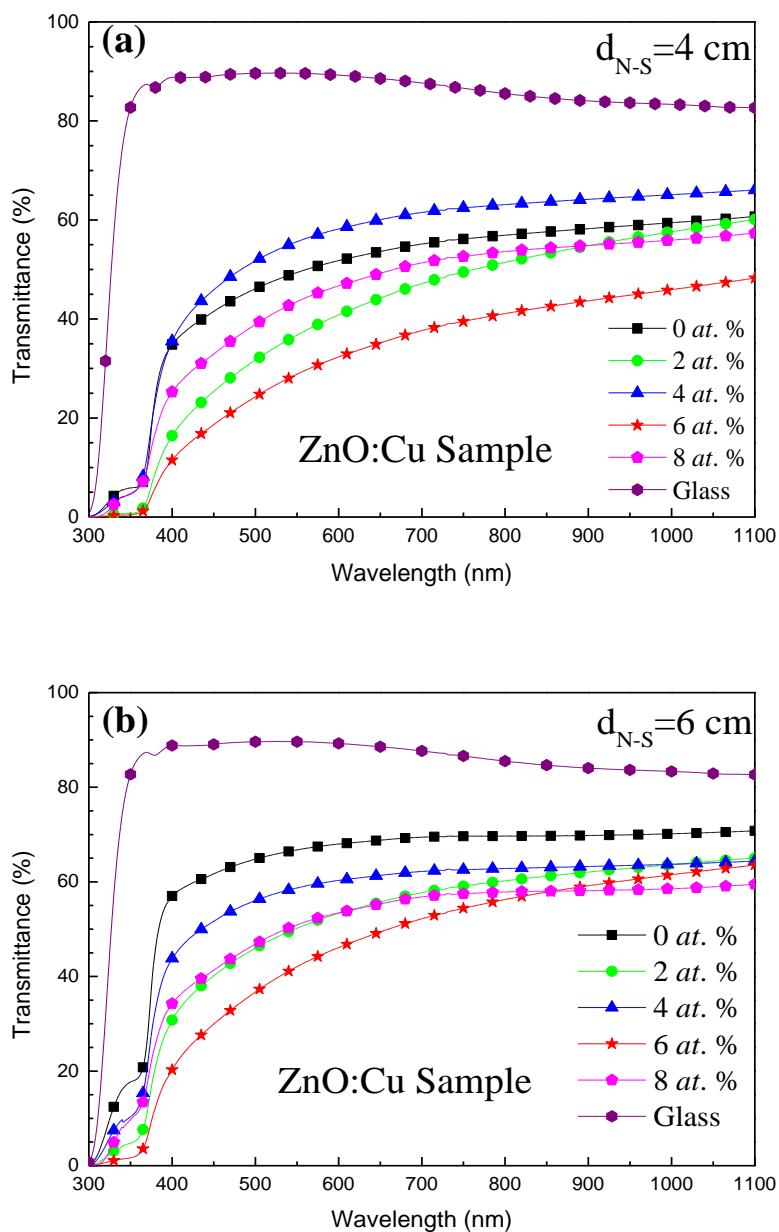
### III.3. Effect the doping with Cu and the distance on the optical transmittance of ZnO thin films.

Figure III.4 represents typical spectra of the change in optical transmittance as a function the wavelength of the incident photon in the UV-Vis-NIR, ZnO:Cu sample with different percentages of doping (0, 2, 4, 6, and 8 at. %) prepared on glass substrate was obtained by ultrasonic spray pyrolysis technique at 300 °C and 0.05 mol/l, under two different distances.

These figures, shows the sensitivity of the samples transmittance to the variation doping and distance. It can be clearly distinguished that all spectra of the transmittance consist of two wavelength ranges:

- ❖ The first region [400-1100 nm], where the samples does not have a high transmittance compared to the transmittance of the glass “90 %” in view of the fact that it absorbed part of the incoming rays where the transmittance values are between 44 % and 65 % at a distance 4 cm (the most transmittance sample when 4 at. %) and it is between 58 % and

70 % at a distance 6 cm (the most transmittance sample when 0 *at. %*). In addition, the transmittance decreases with decreasing wavelength.



**Figure III.4.** Optical transmittance spectra of ZnO:Cu samples prepared at **(a):**  $d_{N-S} = 4$  cm and **(b):**  $d_{N-S} = 6$  cm.

- ❖ The second region [300-400 nm], the transmittance of the sample is weak, it behaves like an opaque material, and this is due to the absorption of ultraviolet rays by the prepared material that help them in the electronic transition, where both the gap energy and the Urbach energy are determined in this region. We notice that the absorption edge (which lies



between the two regions) is red-shifted to the visible region with doping, which indicates the narrowing of the optical band gap.

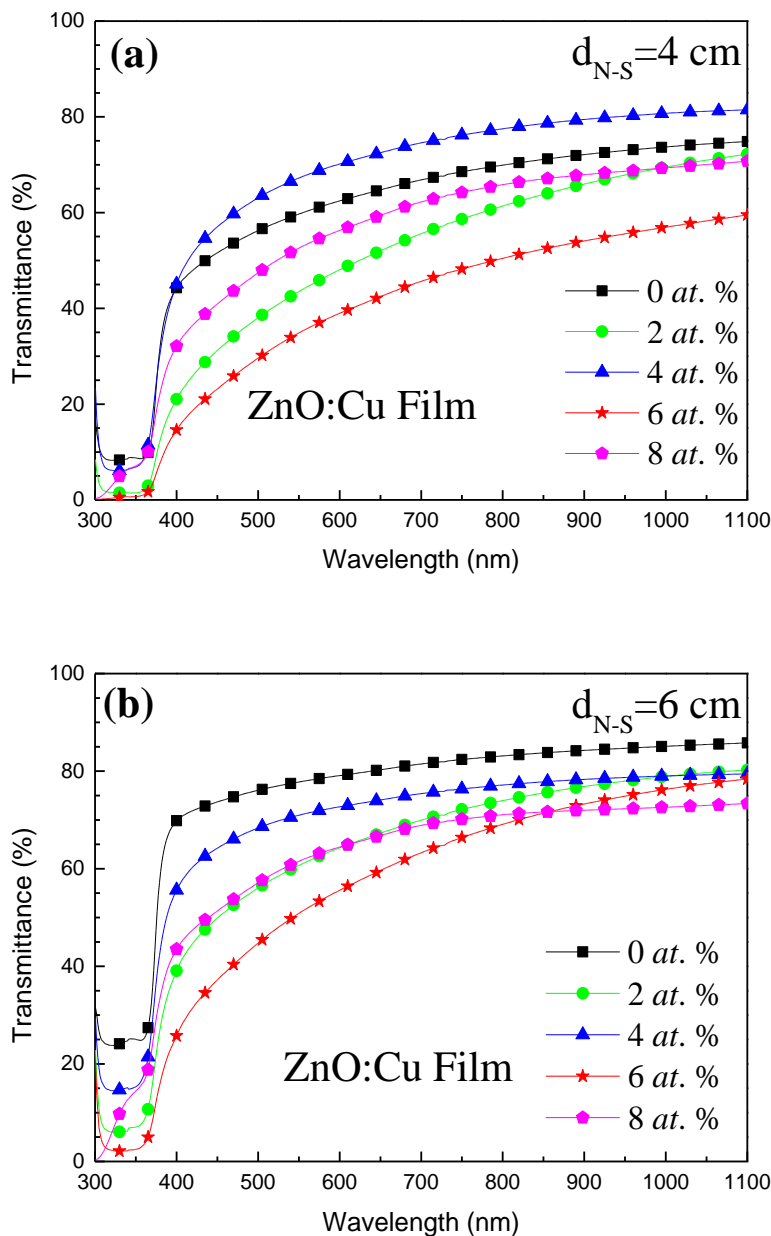


**Figure III.5.** Optical transmittance spectra of ZnO:Cu thin films prepared at (a):  $d_{N-S} = 4$  cm and (b):  $d_{N-S} = 6$  cm.

Figure III.5 (a & b) represents typical spectra of the variation in optical transmittance as a function of the wavelength by the incident photon in the UV-Vis-NIR range, it was obtained by placing the reference glass, so the transmittance of the copper-doped zinc oxide films was recorded only, while neglecting the transmittance of the glass. The transmittance decreases with decreasing wavelength to  $T = 0\%$  at 300 nm, except for undoped ZnO and ZnO:Cu with 4 at. %

( $T_{\lambda=300\text{ nm}} \neq 0$ ) at the same distances, which is due to the possible presence of voids in the thin films [69].

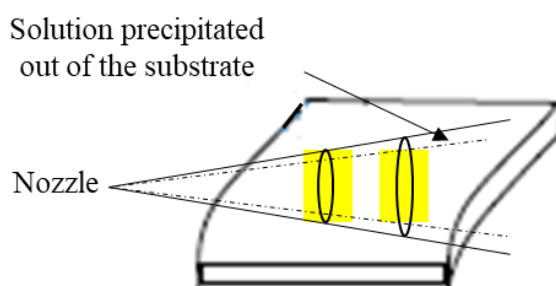
The transmittance values of ZnO are decreases from 80 % to 55 % at  $d_{N-S} = 4$  cm and from 83 % to 68 % at  $d_{N-S} = 6$  cm with increasing doping percentage with Cu. This decrease is due to the presence of Cu atoms in the film (Cu is darker compared to Zn) and the optical transmittance of the ZnO thin films is higher than CuO (Figure II.10).

For  $d_{N-S} = 6$  cm, a special case when doped at 6 *at. %*, its transmittance is less than other films, and this may be due to the roughness of the surface and the presence of a large number of grain boundaries. In contrast, the transmittance for ZnO doped with 4 *at. %* and 8 *at. %* by Cu at  $d_{N-S} = 4$  cm was high permeability and this is due to the small thickness of the film which could be due to the presence of an air current during the preparation which hindered the process of deposition of the solution on the substrate.

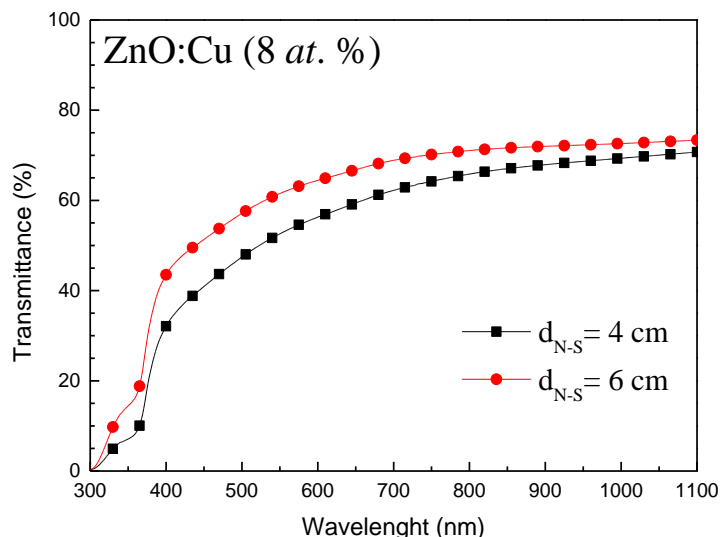
The optical transmittance decreases with decreasing nozzle-substrate distance at the same doping (Figure III.6). We explain this decrease by the fact that when spraying at a distance of 6 cm, less of the base material (Zn, Cu) reaches the substrate and this is linked to the so-called solid angle represented by the figure III.7, therefore the thickness of the films prepared is very thin which allows light penetrates it easily [70]. The percentage of transmittance at a far distance is greater than at a close distance because it allowed enough time to give it to oxygen to penetrate the films.

**Table III.1.** Optical transmittance ZnO:Cu at 600 nm.

ZnO:Cu ( <i>at. %</i> )		0%	2%	4%	6%	8%
Transmittance(%)	$d_{N-S} = 4$ cm	58	45	70	35	54
	$d_{N-S} = 6$ cm	78	66	72	52	64



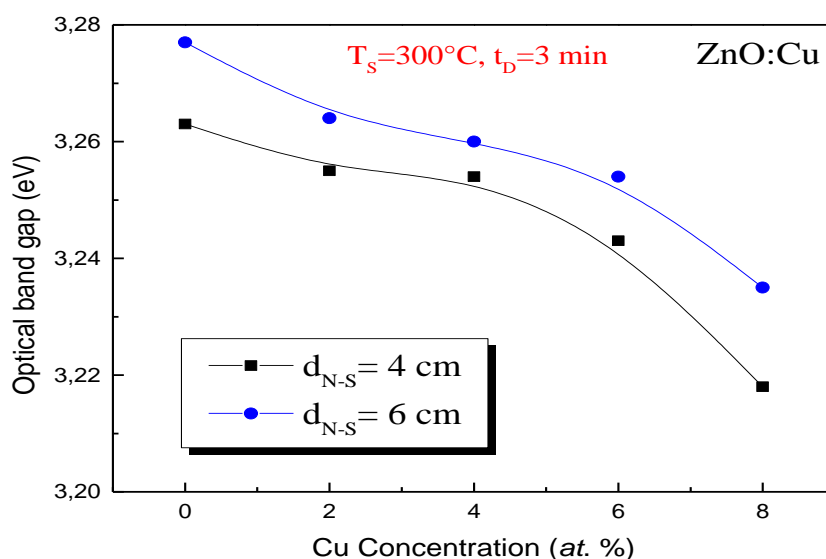
**Figure III.6.** Schematic diagram shows the solution spray from the nozzle to substrate.



**Figure III.7.** Variation of optical transmission of ZnO:Cu (8 at.%) thin films at different Nozzle-Substrate distances.

#### III.4. Effect the doping with Cu and the distances on the optical band gap of the ZnO thin films

The optical gaps were estimated from the spectra the variation of  $(\alpha hv)^2$  as a function of the incident photon energy ( $hv$ ) for the ZnO:Cu thin films deposited by the ultrasonic spray pyrolysis technique on glass substrates for different percentages doping (0, 2, 4, 6, and 8 at. %). We find in each spectrum a part which varies linearly with the incident energy [11,51], indicating that the deposited ZnO:Cu has a single gap optical ( $E_g$ ). This optical gap energy was found from the linear part of this spectrum  $(\alpha hv)^2 = f(hv)$  where  $(\alpha hv)^2 = 0$  [71].



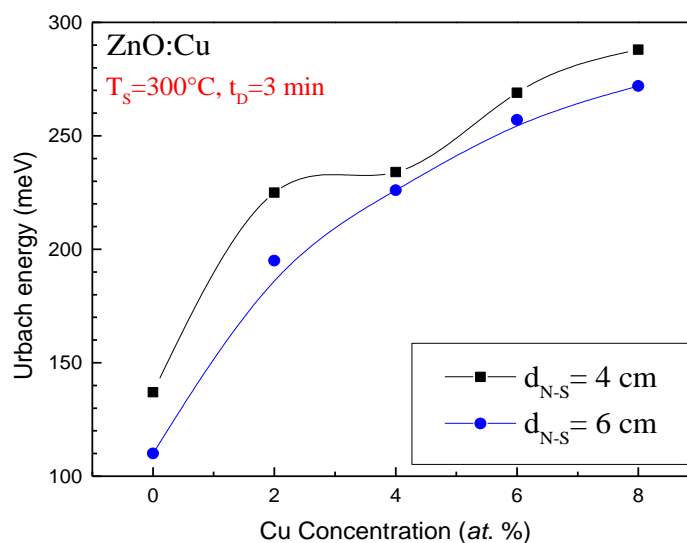
**Figure III.8.** Variation the optical gap energy of ZnO thin films as a function of Cu concentration at two different distances.

Figure III.8 shows the variation of the optical gap energy ( $E_g$ ) as a function of the doping percentage (at %) of ZnO:Cu.

We notice through the curve that the values of the energy gap decrease as we increase the doping by copper, where the energy gap values range between 3.21 eV and 3.26 eV at  $d_{N-S} = 4$  cm and between 3.22 eV and 3.265 eV at  $d_{N-S} = 6$  cm, we explain this decrease due to the substitution of Cu ions in the ZnO structure causing exchange of ions in the conduction band and the valence band which eventually results in the band gap narrowing effect due to Burstein–Moss shift. A similar trend has been observed in pure and Cu doped ZnO thin films in previous reports [72]. There is a possibility as well is due to an increase in the concentration of free electrons. This is, possibly the result the occupation of the interstitial sites by the atoms of the dopant because the latter represent the main donors in the ZnO nanostructures [73].

There is a difference in the energy gap values during preparation with two different distances ( $d_{N-S}$ ), where at the close distance  $d_{N-S} = 4$  cm, it led to the arrival of the solution in a large amount to the substrate, offset by an increase in the main substance amount concentration (Cu and Zn) on the substrate, and therefore  $E_g$  is small, in contrast to the far distance  $d_{N-S} = 6$  cm, it resulted in the arrival of the solution in a small amount. Thus, the number of particles in the crystalline structure is considered, so the formed defects are few, the energy gap is close to the theoretical value at this distance [12].

### III.5. Effect the doping with Cu and distance on the Urbach energy of ZnO thin films



**Figure III.9.** Variation the Urbach energy of ZnO thin films as a function of Cu concentration at two different distances.

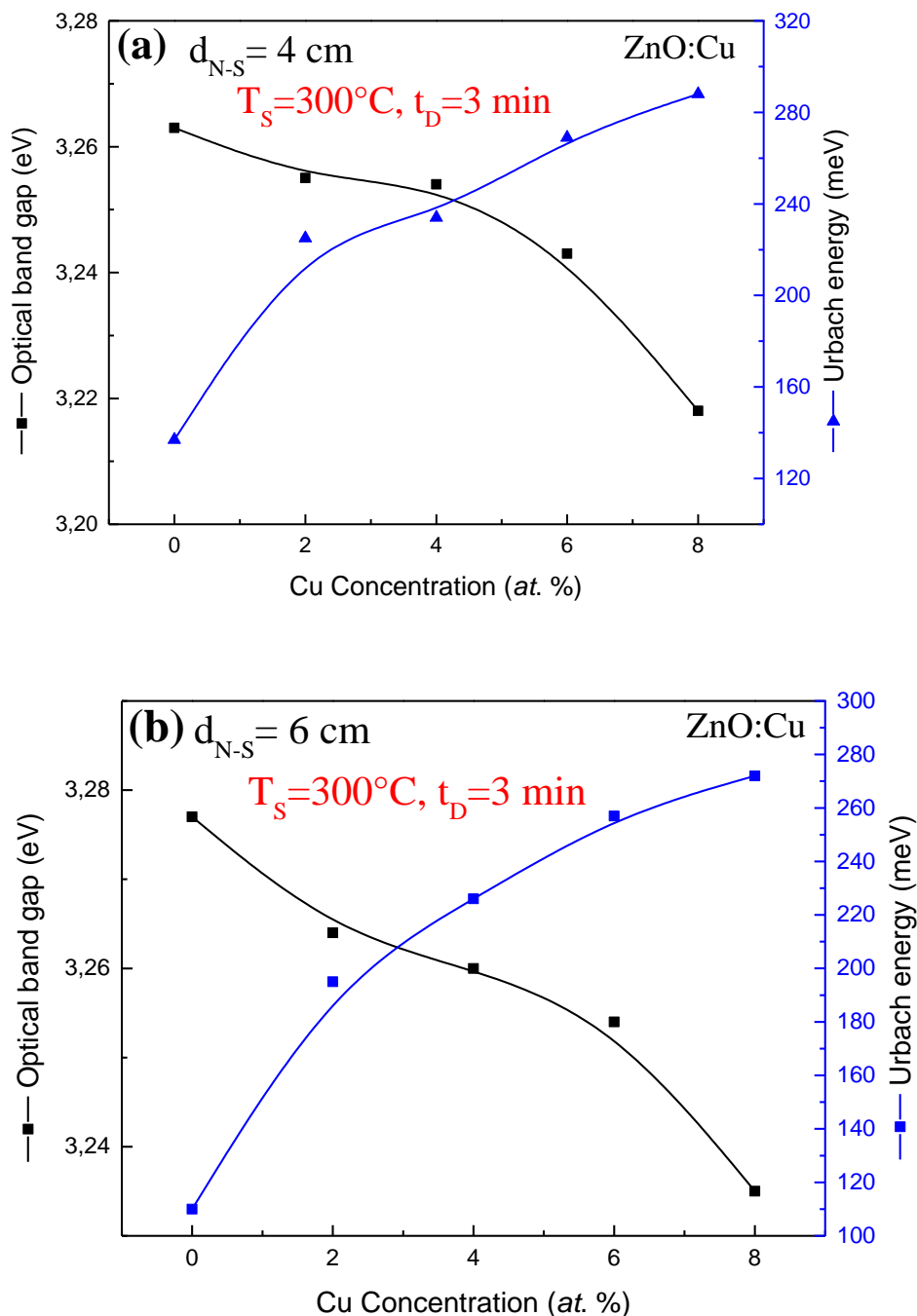
From the spectrum of the variation ( $\ln\alpha$ ) as a function the energy of the incident photon ( $h\nu$ ), we find, in all the samples prepared “ZnO:Cu” at two different distances, a part which varies linearly with the energy of the incident photon. In this part, we can deduce the value of Urbach energy ( $E_{Urb}$ ) which expresses disturbances in the basic structure of the thin slices resulting when these films grow.

Figure III.9 shows the variation of the Urbach energy of ZnO thin films as a function of doping by Cu (0, 2, 4, 6, and 8 *at. %*) which are deposited by ultrasonic spray pyrolysis technique on glass substrates. We note that the Urbach energy is related to the copper concentration. The Urbach energy is increase from 135 meV to 290 meV and from 110 meV to 270 meV for  $d_{N-S} = 4$  cm and  $d_{N-S} = 6$  cm, respectively.

At the same distance, we note the presence of Urbach energy in the sample of undoped zinc oxide, and this is due to the method of preparation (spray pyrolysis), and it increases with increasing the doping by Cu. This behavior can also be attributed to the optical absorption of the material, the diversity of impurities and the presence of defects in the crystal lattice among [24].

At the same doping ratio, the decrease of Urbach energy by increasing the Nozzle-substrate distance ( $d_{N-S}$ ) is explained by a decrease in the amount of material deposited for the same preparation time. Which in turn provides sufficient time for the solution to react, hence a smaller number of defects [10]. Where at the close distance, Urbach energy is great due to the large number of defects, including the lack of uniformity. The incorporation of impurities or disorders and defects in the semiconductors leads to local electric fields which affect the tape tails near the edge of the tape [24,67].

The figure III.9 (a and b) show the inverse relationship between the optical band gap and Urbach energy as a function of copper concentration prepared at two deferent distances nozzle-substrate (4 cm and 6 cm).



**Figure III.10.** Variation of Urbach energy and gap energy of ZnO:Cu thin films as a function of doping percentage in; (a) 4cm, (b) 6cm.

### III.6. Effect the doping with Cu and nozzle distance on the refractive index of ZnO thin films

The refractive index ( $n$ ) can be determined by fitting a calculated transmittance curve, according to a model proposed by Swanepoel to the measured transmittance spectrum.

Figure III.11 shows the variation of refractive index to the ZnO thin films for different rates of doping by Cu at two different distances nozzle-substrate.

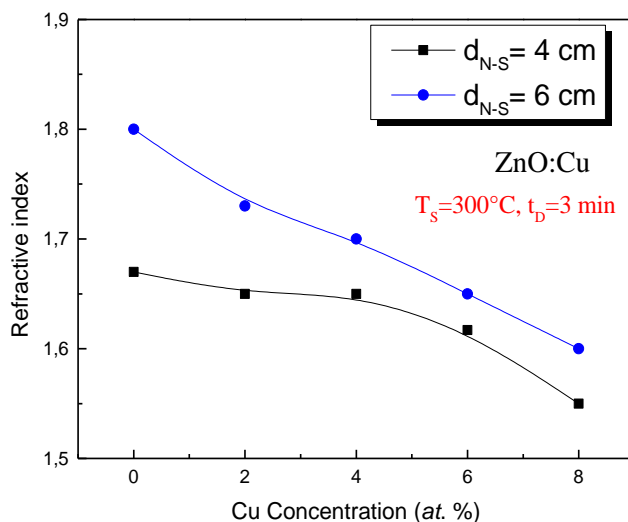


**Figure III.11.** Variation the refractive index of ZnO thin films as a function of Cu concentration at two different distances.

We notice that the refractive index values of ZnO decrease from 1.8 to 1.6 at  $d_{N-S} = 6$  cm and from 1.67 to 1.55 at  $d_{N-S} = 4$  cm with the increasing Cu doping level from 0 to 8 at. %.

We explain this decrease due to the increase in the number or size of porosity in the prepared film, which leads to obtaining a less dense material, and this is by increasing the copper concentration as a doped for zinc oxide [24,74]. It is known that the refractive index is the ratio between the speed of light in a vacuum and its speed in a medium, so in the presence of voids that allow the passage of light easily and its speed increases. From this the refractive index decreases. Where, there is an inverse relationship between film thickness and refractive index (Figure III.12).

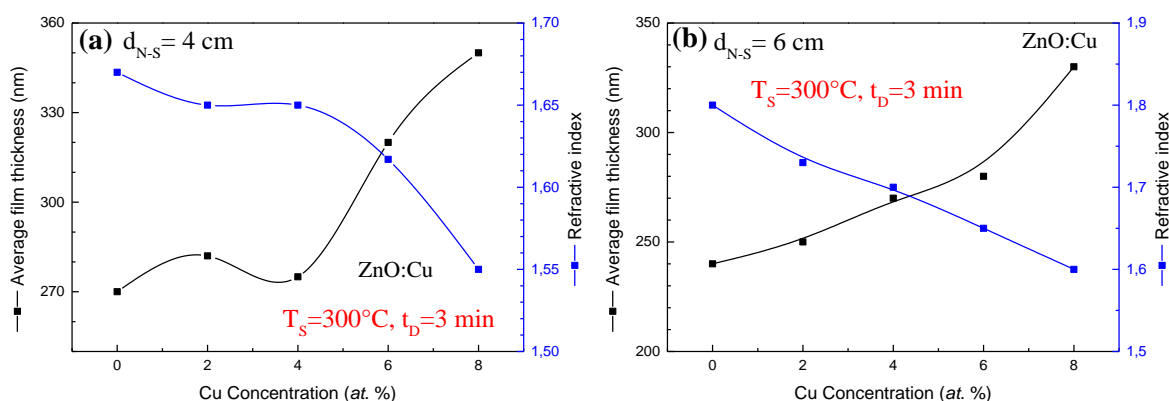


**Figure III.12.** Variation of thickness and refractive index of ZnO thin films versus Cu concentration prepared at: (a) 4cm, (b) 6cm.

### III.8. Effect the doping with Cu and the distance on electrical conductivity of ZnO thin films

The electrical properties of thin films of metal oxide such as ZnO, CuO, and Cu<sub>2</sub>O are of considerable interest in several industrial applications such as photovoltaic cells, gas sensors, and lithium batteries. Among these properties, the electrical conductivity as the most important parameter [18,23].

ZnO:Cu thin films on glass substrate were prepared by ultrasonic spray pyrolysis technique using in order to determine of the electrical properties, we use the four-probe method, which determining the sheet resistance ( $\Omega/\square$ ), it calculated as follows [10]:

$$\rho_s = \frac{\pi V}{\ln 2 I} \quad \text{III.1}$$

In the above said configuration, a correction factor of  $\frac{\pi}{\ln 2} = 4.53$  was applied for the sample. Figure III.13 shows the variation of electrical conductivity of ZnO thin films with Cu concentration at two different nozzle-substrate distances.

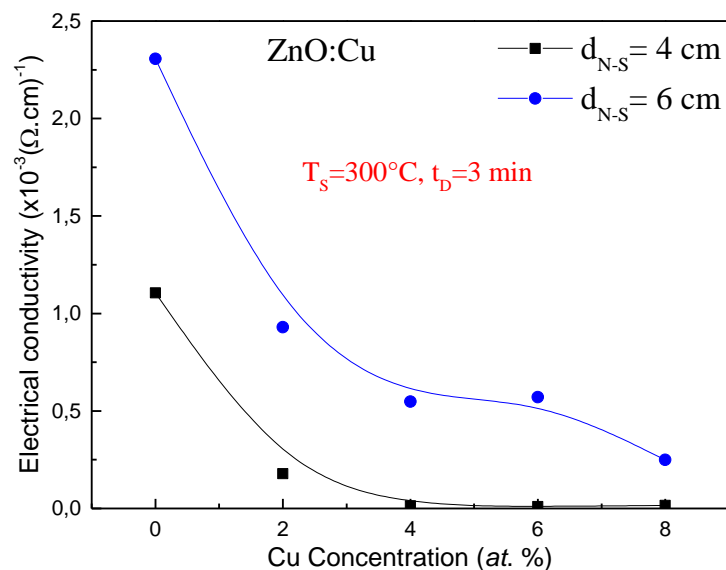



**Figure III.13.** Variation of electrical conductivity of ZnO:Cu thin films at two different distances.

The electrical conductivity values of ZnO are decreases from  $2.30 \times 10^{-3}$  to  $0.25 \times 10^{-3} (\Omega \cdot \text{cm})^{-1}$  at  $d_{N-S} = 6$  cm and from  $1.10 \times 10^{-3}$  to  $0.016 \times 10^{-3} (\Omega \cdot \text{cm})^{-1}$  at  $d_{N-S} = 4$  cm with increasing doping percentage with Cu. We explain these decreases:



At the same doping, this decrease of electrical conductivity as the substrate approaches the spray nozzle is associated with an increase the number of grain boundaries that impede the mobility of electrons inside the thin film (equation I.1), in addition to the presence of ionized impurity and the existence of defects in the films increases the probability of free carrier collisions and the vibration of the atoms of the crystal lattice around their equilibrium position is also an obstacle for free electrons [53,75].

At the same distance between the nozzle and the substrate, the decrease of electrical conductivity is due to the substitution of copper ions in the zinc oxide matrix, where the copper oxide is p-type semiconductor unlike for zinc oxide (n-type) [75], Therefore, the percentage of oxygen increases in the material when the zinc atoms are replaced with copper atoms and maintains the type of semiconductor of ZnO, which allows a decrease in free charge carrier (electrons) in the material.



# General conclusion

"ONE OF THE BASIC RULES OF  
THE UNIVERSE IS THAT  
**NOTHING IS PERFECT.**  
**PERFECTION SIMPLY DOESN'T EXIST...**  
WITHOUT IMPERFECTION,  
NEITHER YOU NOR I  
WOULD EXIST."  
*-STEPHEN HAWKING*



HUFF  
POST

JETHO BALLUJA VIA GETTY IMAGES

## General conclusion

The steer of this study is to develop zinc oxide thin films by ultrasonic spray pyrolysis technique on glass substrates and study the effect of Cu concentration and nozzle-substrate distance on the optical and electrical properties of these samples. This technique of making materials is very attractive, simple, easy to control, and low-cost chemical technique. On the other hand, the thin films obtained are good quality and have excellent adhesion.

Copper-doped zinc oxide thin films (ZnO:Cu) were deposited onto glass substrates with different doping rate (0, 2, 4, 6, and 8 *at. %*) from an aqueous solution of zinc acetate dihydrate and copper chloride dihydrate at two different nozzle-substrate distances (4 cm and 6 cm). Molar concentration, substrate temperature, flow rate and spray time were maintained constant throughout the deposition process at 0.05 mol/l, 300 °C, 60 ml/h, and 3 min, respectively. The obtained samples are characterized by UV-Visible-NIR spectrophotometer and four probe technique to determine their optical and electrical properties. The characterization of the films leads us to the following conclusions:

With increase the Cu concentration, we observe the color of our samples is change (from lighter to darker). This variation is due to the increase of both of crystal defects, impurities, and grains boundaries in addition to the substitution of copper ions in the zinc oxide matrix resulting in a decrease in the number of charge carriers and their mobility.

With increase the nozzle-substrate distance at the same doping by Cu, all the properties of the prepared films improve, become more transparent to light and conducts electricity that the value of its energy gap becomes close to the theoretical value. In addition, a lower Urbach energy indicates a decrease in crystalline defects which means that the films are more stable and crystallized.

**References**

- [1] F. Ynineb, Contribution à l'élaboration de couches minces d'Oxydes Transparents Conducteurs (TCO), Magister Memory, Mentouri Brother University, Constantine-2010.
- [2] M. Dahnoun, Preparation and characterization of titanium dioxide and zinc oxide thin films via sol-gel technique for optoelectrical applications, Doctoral Thesis (LMD), Mohamed khider University, Biskra -2020.
- [3] B. Chermime, Caractérisation des revêtements MoVN déposés sur les substrats XC100 et Si par pulvérisation cathodique magnétron, Doctoral Thesis, Batna 2 University, Batna-2017.
- [4] L. Herissi, Élaboration par pulvérisation pyrolytique et caractérisation de couches minces semiconductrices et transparentes d'oxyde de zinc : Perfectionnement du système de dépôt, Magester Thesis, Larbi Ben M'hidi University, Oum El Bouaghi-2008.
- [5] L. Hafsa, L. Hadjeris, L. Herissi, UV-induced photocatalytic degradation of methyl green dye by ZnO nanowires and nanorods obtained by spray pyrolysis, Nano Hybrids and Composites 36 (2022) 69.
- [6] S. Bouchrit, A. Sari, Elaboration et caractérisation du couche minces d'oxyde de cuivre, Master Memory, Larbi Tebessi University, Tebessa-2017.
- [7] R. Bacha, La synthèse des nano particules de CuO avec la méthode de précipitation sol-gel, en utilisant le précurseur  $\text{CuCl}_2$  et l'étude de leurs propriétés structurales et optiques, Doctoral Thesis, Mentouri Brother University, Constantine-2015.
- [8] A. Boughelout, Elaboration et caractérisation de couches minces d'oxyde de zinc dopées aux métaux pour des applications photovoltaïques et en détection de gaz, Doctoral Thesis, Houari Boumediene University, Algiers-2019.
- [9] M. Mosca, R. Macaluso, C. Cali, R. Butté, S. Nicolay, E. Feltin, D. Martin, N. Grandjean, Optical, structural, and morphological characterisation of epitaxial ZnO films grown by pulsed-laser deposition, Thin Solid Films 53 (2013) 55.
- [10] B. Maatoub & S. Fiseh, Study of the optical and Electrical properties of tin oxide thin films deposited by spray pyrolysis technique, Master Memory, Larbi Tebessi University, Tebessa-2021.

- [11] D. Rahal & T. Zerfaoui, Elaboration of tin dioxide thin films by spray pyrolysis using different concentrations of solution and solvent, Master Memory, Larbi Tebessi University, Tebessa-2022.
- [12] L. Herissi, Élaboration et caractérisation de couches minces d'oxydes métalliques destinées à des applications optoélectroniques, Doctoral Thesis, Larbi Ben M'hidi University, Oum El Bouaghi-2016.
- [13] A.A. Bensekhria, Élaboration de couches minces de ZnO:V transparentes conductrices à basse pression et à pression atmosphérique pour applications photovoltaïques, National Institute for Scientific Research, Quebec University, Canada-2020.
- [14] M. TOUATI TLIBA, Etude des propriétés optiques et électroniques des couches minces de ZnO dopé et non dopée : élaboration et application, Master Memory, Kasdi Merbah University, Ouargla-2019.
- [15] J. DSY, N. Peiris TA, Overview on transparent conducting oxides and state of the art of low-cost doped ZnO systems, SF Journal of Material and Chemical Engineering. 1 (2018) 1004.
- [16] B. Astuti, A. Zhafirah, V.A. Carieta, N. Hamid, P.Marwoto, Sugianto, U.Nurbaiti, F.D Ratnasari, N.M. Putra, D. Aryanto, X-ray diffraction studies of ZnO:Cu thin films prepared using sol-gel method, Journal of Physics Conference Series 1567 (2020) 22004.
- [17] H. Meddas, Effet du dopage par l'azote sur les propriétés des films minces de d'oxyde de titane préparé par procède sol-gel, Master Memory, Mohamed khider University, Biskra -2020.
- [18] N. Menasria, H. Talbi, Elaboration et caractérisation de couche minces d'oxyde de cuivre dopée par zinc cuivre, Master Memory, Larbi Tebessi University, Tebessa-2017.
- [19] A. Ferdi, A. Hafdallah, B. Harkati, L. Herissi, Effect of Zn doping on the structural and optical properties of NiO thin films deposited by spray pyrolysis technique, Functional Materials 28 (2021) 669.
- [20] L. Herissi L. Hadjeris, M.S. Aida, J. Bougdira, Properties of  $(\text{NiO})_{1-x}(\text{ZnO})_x$  thin films deposited by spray pyrolysis, Thin Solid Films 605 (2016) 116.
- [21] J. Garnier, Elaboration de couches minces d'oxydes transparents et conducteurs par spray CVD assiste par radiation infrarouge pour applications photovoltaïques, Doctoral Thesis, National School of Arts and Crafts, Morocco-2009.

- [22] M. Othmane, Synthesis and characterization of Zinc Oxide (ZnO) Thin films deposited by spray pyrolysis for applying: electronics and photonics, Doctoral Thesis, Mohamed Khider University, Biskra-2018.
- [23] A. Belaoura, Étude de l'effet du dopage par Sn sur les propriétés des couches minces de ZnO, Master Memory, Larbi Tebessi University, Tebessa-2016.
- [24] H. Slimi, Elaboration et caractérisation de couches minces co-dopées In, Co, préparées par la pulvérisation cathodique, applications aux cellules photovoltaïques, Doctoral Thesis, Sfax University, Tunisia-2019.
- [25] D. Allouane, Elaboration de couches minces d'oxyde de zinc par pulvérisation pyrolytique destinées à des applications optoélectroniques, Magester Thesis, Larbi Ben M'hidi University, Oum El Bouaghi-2010.
- [26] Y. Aoun, B. Benhaoua, B. Gasmi, & S. Benramache, Structural, optical and electrical properties of zinc oxide (ZnO) thin films deposited by a spray pyrolysis technique, Journal of Semiconductors 36 (2015) 1.
- [27] A. Taabouche, Contribution à l'étude structurale et microstructurale de films ZnO obtenus par ablation laser, Magister Thesis, Mentouri Brother University, Constantine-2010.
- [28] S. Rajeh, A Barhoumi, A. Mhamdi, G Leroy, B Duponchel, M Amlouk and S.Guermazi, Structural, morphological, optical and opto-thermal properties of Ni doped ZnO thin films using spray pyrolysis chemical technique, Bulletin of Materials Science 39 (2016) 177.
- [29] E. H. Kennard and E. O. Dieterich, An effect of light upon the contact potential of selenium and cuprous oxide, Physical Review 9 (1917) 58.
- [30] N. Abdelmalek, L. Hadjeris, D. Allouane, L.Herissi, S. Rahmane & H. Moualki, Structural, Optical and Electrical Properties of ZnO: Fe Thin Films Grown by Spray Pyrolysis, Journal of New Technology and Materials 04 (2014) 47.
- [31] M. Lamri Zeggar, Cupric oxide thin films deposition for gas sensor application, Doctoral Thesis, Mentouri Brother University, Constantine-2016.
- [32] S. Koussi Daoud, Préparation électrochimique et caractérisation de couches nanostructures de semi-conducteurs de type p pour cellules photovoltaïques hybrides, Doctoral Thesis, Pierre et Marie Curie University, France-2016.

- [33] K. Medjnoun, Etude et réalisation de semi-conducteur transparents ZnO dopé vanadium et oxyde de vanadium en couches minces pour application photovoltaïques, Doctoral Thesis, Mouloud Mammeri University, TiziOuzou-2015.
- [34] M. Heinemann, B. Eifert, and C. Heiliger, Band structure and phase stability of the copper oxides Cu<sub>2</sub>O, CuO, and Cu<sub>4</sub>O<sub>3</sub>, *Physical Review B* 87 (2013) 115111.
- [35] K. Limkraisiri, Copper oxide by thermal oxidation for electrochemical cells and gas sensors, Doctoral Thesis, University of California, Californie-2013.
- [36] Y. Wang, Controllable growth, Microstructure and electronic structure of copper oxide thin films, Doctoral Thesis, Lorraine University, France-2015.
- [37] S. S. Shariffudin, S. S. Khalid, N. M. Sahat, M. S. P. Sarah, H. Hashim, Preparation and Characterization of nanostructured CuO thin films using Sol-gel Dip Coating, *Materials Science and Engineering* 99 (2015) 12007.
- [38] Y. Benkhetta, L'effet du débit de la solution sur les propriétés des couches minces d'oxyde de zinc (ZnO) déposées par spray ultrasonique, Memory Thesis, Mohamed Khider University, Biskra-2013.
- [39] J.E. Greene, Chapter 12: Thin film nucleation, growth, and microstructural evolution: An atomic scale view, *Science, Applications and Technology*, (2010) 554.
- [40] K. Wasa, M. Kitabatake, H. Adachi, Thin film materials technology-Sputtering of Compound Materials, William Andrew publishing 1 (2004) 102.
- [41] A. Aldrin, Preparation and characterization of certain II-VI, I-III-VI<sub>2</sub> semiconductor thin films and transparent conducting oxides, PhD thesis, Cochin University, India-2004.
- [42] Y. Larbah, Elaboration et caractérisation des couches minces conductrices et transparentes pour les cellules solaires de type TCO/ZnS/CIS, Magister Thesis, Mohamed Boudiaf University, Oran-2011.
- [43] M. Tadatsugu, I. Satoshi, M Toshihiro, M. Youhei, Transparent conducting ZnO thin films deposited by vacuum arc plasma evaporation, *Thin Solid Films* 445 (2003) 268.
- [44] S. Redjel & N.H. Mekhaznia, Elaboration and characterization of tin oxide thin films deposited by spray pyrolysis, Memory Thesis, Larbi Tebessi University, Tebessa-2020.

- [45] R. Zamiri, B. Singh, D. Dutta, A. Reblo, J. Ferreira, Electrical properties of Ag-doped ZnO nano-plates synthesized via wet chemical precipitation method, *Ceramics International* 40 (2014) 4471.
- [46] C. Kelifi, Tin dioxide SnO<sub>2</sub> thin films deposited by ultrasonic spray technique: Properties and applications, Doctoral Thesis, Mohamed Khider University, Biskra-2018.
- [47] M. A. Aegerter, J. Puetz, G. Gasparro & N. Al-Dahoudi, Versatile wet deposition techniques for functional oxide coatings, *Optical Materials* 26 (2004) 155.
- [48] G. Srinivasan, N. Gopalakrishnan, Y. S. Yu; R. Kesavamoorthy, J. Kumar, Influence of post-deposition annealing on the structural and optical properties of ZnO thin films prepared by sol-gel and spin-coating method, *Superlattices and Microstructures* 43 (2008) 112.
- [49] R. Scheer, K. Diesner, H. J. Lewerenz, Experiments on the microstructure of evaporated CuInS<sub>2</sub> thin films, *Thin Solid Films* 268 (1995) 130.
- [50] H. Moualkia, N. Attaf, L. Hadjeris, L. Herissi and N. Abdelmalek, Investigation on chemical bath deposited CdS thin films, *Journal of New Technology and Materials* 01 (2011) 47.
- [51] S. Guellati, C. Boussahla, Étude de l'effet de dopage par nickel et du recuit sur les propriétés des couches minces d'oxyde de cuivre, Master Memory, Larbi Tebessi University, Tebessa-2019.
- [52] A. Ashok, G. Regmi, S. Velumani, Growth of In<sub>2</sub>Se<sub>3</sub> thin films prepared by the pneumatic spray pyrolysis method for thin film solar cells applications, 17<sup>th</sup> International Conference on Electrical Engineering, Computing Science and Automatic Control (CCE), Mexico, 2020.
- [53] L. Hadjeris, L. Herissi, M. Assouar, T. Easwarakhanthan, J. Bougdira, N. Attaf and M S. Aida, Transparent and conducting ZnO films grown by spray pyrolysis, *Semiconductor Science and Technology* 24 (2009) 035006.
- [54] SR. Ardecani, ASR Aghdam, M Nazari & A Bayat, A comprehensive review on ultrasonic spray pyrolysis technique: Mechanism, main parameters and applications in condensed matter, *Journal of analytical and applied pyrolysis* 141 (2019) 104631.
- [55] L. Eckertová, Chapter 4: Mechanism of film formation, *Physics of thin films* (1977) 72.
- [56] G. Zhu, T. Lv, L. Pan, Z. Sun, & C. Sun, Changqing All spray pyrolysis deposited CdS sensitized ZnO films for quantum dot-sensitized solar cells. *Journal of Alloys and Compounds* 509 (2011) 362.



- [57] V.K. Singh, Thin film deposition by spray pyrolysis techniques, *Journal of Emerging Technologies and Innovative Research* 4 (2017) 910.
- [58] Z. Ghorannevis, M. T. Hosseinnejad, M. Habibi & P. Golmahdi, Effect of substrate temperature on structural morphological and optical properties of deposited Al/ZnO films, *Journal of Theoretical and Applied Physics* 9 (2015) 33.
- [59] B. Abdallah, A. Ismail, H. Kashoua, and W. Zetoun, Effects of deposition time on the morphology, structure, and optical properties of PbS thin films prepared by chemical bath deposition, *Journal of Nanomaterials* 2018 (2018) 1826959.
- [60] A. Djelloul, Etude des propriétés morphologiques, structurales et optiques des couches de CdS, ZnS et CIS pour application cellules solaires de type métal/TCO/CdS/CIS, Doctoral Thesis, Mohamed Boudief University, Oran-2017.
- [61] Z. Moussa, L. Hadjeris, L. Herissi, N. Attaf, N. Moussa, Zn-doped iron oxide thin films prepared by spray pyrolysis technique and characterized for use as an efficient photocatalyst for methyl green organic dye, *Nano Hybrids and Composites* 35 (2022) 95.
- [62] C. Khelifi, Tin dioxide SnO<sub>2</sub> thin films deposited by ultrasonic spray technique: Properties and applications, Doctoral Thesis, Mohamed Khider University, Biskra-2018.
- [63] T. Fukumura, Z. Jin, M. Kawasaki, T. Shono, T. Hasegawa, S. Koshihara, H. Koinuma, *Applied Physics Letters*. 78 (2001) 958.
- [64] S. Roy, S. Basu, Improved zinc oxide film for gas sensor applications, *Bulletin of Materials Science* 25 (2002) 513.
- [65] S. Hariach, N. Attaf, L. Herissi, J. Bougdira, H. Rinnert, M.S. Aida, Cu<sub>x</sub>S thin films deposited by chemical bath, 12<sup>th</sup> Moroccan Meeting on Solid State Chemistry, Morocco-2012.
- [66] L. Herissi, L. Hadjeris, M.S. Aida, S. Azizi, A. Hafdallah and A. Ferdi, Ni-doped ZnO thin films deposited by pneumatic spray pyrolysis, *Nano Hybrids and Composites* 27 (2019) 21.
- [67] L. Herissi, L. Hadjeris, H. Moualkia, N. Abdelmalek, N Attaf, M. S. Aida, J. Bougdira, Realization and study of ZnO thin films intended for optoelectronic applications, *Journal of New Technology and Materials* 1 (2011) 39.
- [68] R. Swanepoel, Determination of the thickness and optical constants of amorphous silicon, *Journal of Physics E: Scientific Instruments* 16 (1983) 1214.

- [69] F.Z. Ababsia & S. Fares, *Élaboration et caractérisation des couches minces d'oxyde de nickel dopé au cuivre*, Master Memory, Larbi Tebessi University, Tebessa-2018.
- [70] E.U. Masumdar, M.A. Barote, Structural, morphological and optical properties of spray deposited nanocrystalline ZnO thin films: Effect of nozzle to substrate distance, *Sensors & Transducers Journal* 146 (2012) 164.
- [71] A.D. Saragih, H. Abdullah and D.-H. Kuo, Study on the doping effect of Cu-doped ZnO thin films deposited by co-sputtering technique, *Journal of Physics* 1230 (2019) 012031.
- [72] V. Ganesh, G.F. Salem, I.S. Yahia, and F. Yakuphanoglu Synthesis, Optical and Photoluminescence Properties of Cu-Doped ZnO Nano-Fibers Thin Films: Nonlinear Optics, *Journal of Electronic Materials* 47 (2018) 1798.
- [73] S. Benamrache, *Elaboration et caractérisation des couches minces de ZnO dopées cobalt et indium*, Doctoral Thesis, Mohamed Khider University, Biskra-2012.
- [74] S. Ozharar, E. Ozugurlu, L. Arda, D. Akcan, The effects of Co/Cu Co-doped ZnO thin films: An optical study, *Journal of Alloys and Compounds* 797 (2019) 253.
- [75] B. Khalfallah, I. Riahi, F. Chaabouni, Effect of Cu doping on the structural, optical and electrical properties of ZnO thin films grown by RF magnetron sputtering: Application to solar photocatalysis, *Optical and Quantum Electronics* 53 (2021) 238.

## تأثير التطعيم بالنحاس على الخصائص الضوئية والكهربائية للشرائح الرقيقة لأكسيد الزنك المترسبة بتقنية الرش بالانحلال الحراري

### ملخص

الهدف من هذا العمل هو دراسة تأثير التطعيم بالنحاس والمسافة بين المرذاذ والركيزة على الخصائص البصرية والكهربائية لشرائح أكسيد الزنك الرقيقة من أجل الحصول على خصائص كهروضوئية تؤهلها للاستخدام في العديد من التطبيقات التكنولوجية.

في هذا العمل، قمنا بتحضير أغشية رقيقة من أكسيد الزنك المطعم بالنحاس ( $ZnO:Cu$ ) بنسب ذرية مختلفة (0، 2، 4، 6، و 8٪) على ركائز زجاجية باستخدام تقنية الرش بالانحلال الحراري بواسطة الموجات فوق الصوتية انطلاقاً من محلول خلاصات الزنك ثنائي الهيدرات ومحلول كلوريد النحاس ثنائي الهيدرات وهذا في ظروف تحضير ثابتة (درجة حرارة الترسيب، زمن الترسيب، التركيز المولي ومعدل التدفق للمحلول)، شخّصت هذه العينات باستعمال مطيافية الأشعة فوق البنفسجية-المرئية-القريبة من تحت الحمراء وتقنية المسابير الأربعة لدراسة خصائصهم الضوئية والكهربائية، لاحظنا أن هذه الخصائص تتأثر بتغير تركيز النحاس وكذلك المسافة بين المرذاذ والركيزة. إذ أن زيادة تركيز النحاس أو اقتراب الركيزة من فوهة الرش أثناء التحضير أدى إلى انخفاض كل من النفاذية، معامل الانكسار، فجوة النطاق والناقلية الكهربائية للشرائح مع زيادة كل من سمك وطاقة أورباخ لهذه الشرائح.

**الكلمات المفتاحية:** شرائح رقيقة من  $ZnO:Cu$ ، الرش بالانحلال الحراري، المسافة بين المرذاذ والركيزة، الشفافية، عرض عصابة الطاقة، الناقلية الكهربائية.

# Effet du dopage au Cu sur les propriétés optiques et électriques des couches minces de ZnO déposées par la technique de spray pyrolyse

## Résumé

Le but de ce travail est d'étudier l'effet du dopage au cuivre et de la distance bec-substrat sur les propriétés optiques et électriques des couches minces d'oxyde de zinc pour obtenir des propriétés photoélectriques qui en font un candidat important dans de nombreuses applications technologiques.

Dans ce travail, nous avons préparé des couches minces d'oxyde de zinc dopé au cuivre (ZnO:Cu) à différents pourcentages de dopage (0, 2, 4, 6, 8 % *at.*) sur des substrats en verre par la technique de spray pyrolyse ultrasonique à partir d'une solution d'acétate de zinc d'hydraté et solution de chlorure de cuivre d'hydraté avec des conditions de préparation constantes (température de dépôt, temps de dépôt, concentration molaire et débit de la solution). Ces échantillons ont été caractérisés en utilisant la spectrophotomètre UV-Visible-NIR et la technique des quatre points pour étudier leurs propriétés optiques et électriques.

Nous avons remarqué que ces propriétés sont affectées par la modification de la concentration de cuivre et la distance entre le bec et le substrat. Lorsque, en augmentant la concentration de Cu ou l'approche du substrat au bec de pulvérisation pendant la préparation, la transparence optique, l'indice de réfraction, la bande interdite et la conductivité électrique des films diminuent avec l'augmentation de l'épaisseur et de l'énergie d'Urbach de ces films.

**Mots-clés:** Couches minces de ZnO:Cu, spray pyrolyse, distance bec-substrat, transmittance, gap optique, conductivité électrique.

## **Effect of Cu doping on optical and electrical properties of ZnO thin films deposited by spray pyrolysis technique**

### **Abstract**

The aim of this work is to study the effect of copper doping and nozzle-substrate distance on the optical and electrical properties of zinc oxide thin films to obtain photoelectric properties which makes it an important candidate in many technological applications.

In this work, we have prepared copper-doped zinc oxide thin films (ZnO:Cu) at different atomic percentage (0, 2, 4, 6, 8 *at. %*) onto glass substrates by ultrasonic spray pyrolysis technique from zinc acetate dehydrate solution and copper chloride dihydrate solution with constant preparation conditions (deposition temperature, deposition time, molar concentration and flow rate of solution). These samples were characterized using the UV-Visible-NIR spectrophotometer and the four-probe technique to study their optical and electrical properties.

We notice that these properties are affected by the copper concentration and the nozzle-substrate distance. Where, by increases the Cu concentration or the approach of the substrate to the spray nozzle during preparation, the transmittance, refractive index, band gap, and electrical conductivity of the films are decrease with increasing the both of the thickness and Urbach energy of these films.

**Key-words:** ZnO:Cu thin films, Spray pyrolysis, Nozzle-Substrate distance, Transmittance, optical band gap, electrical conductivity.